Research Square

Preprints are preliminary reports that have not undergone peer review.
They should not be considered conclusive, used to inform clinical practice,
or referenced by the media as validated information.

Thermodynamic and Synoptic Regulations of Thunderstorm Activity in Southern Iraq: A 1990-2019 Examination of Jet Stream Dynamics and Instability Indices

Imad Al-Khulaifawi

imadjasim900@gmail.com

Southern Federal University

Aqeel Ghazi Mutar

Mustansiriyah University

Research Article

Keywords: Thunderstorm, Atmospheric stability, K-index, Total Totals index, CAPE, Temperature, Basra Airport

Posted Date: May 26th, 2026

DOI: https://doi.org/10.21203/rs.3.rs-9059637/v1

License: This work is licensed under a Creative Commons Attribution 4.0 International License.
Read Full License

Additional Declarations: No competing interests reported.

Version of Record: A version of this preprint was published at Meteorology and Atmospheric Physics on October 27th, 2026. See the published version at https://doi.org/10.1007/s00703-026-01222-y.

Thermodynamic and Synoptic Regulations of Thunderstorm Activity in Southern Iraq: A 1990-2019 Examination of Jet Stream Dynamics and Instability Indices

Imad Abdulridha Jasim Al- Khulaifawi [1*]

Aqeel Ghazi Mutar[2]

[1]Department of Oceanology, Institute of Earth Sciences, Southern Federal University, Russia

[2]Department of Atmospheric Sciences, College of Science, Mustansiriyah University, Iraq

imadjasim900@gmail.com / al-@sfedu.ru

https://orcid.org/0009-0008-1610-9795

Abstract: The meteorological phenomenon known as thunderstorms happens due to atmospheric instability. During thunderstorms, there are abrupt changes in temperature, wind speed, atmospheric pressure, rain, and hail. This work assesses thunderclouds in terms of structure, physical characteristics, and accompanying atmospheric stability indicators and attempts to develop statistical classifications of thundercloud frequencies in the city of Basra. The data for the duration from 1990 to 2019 was obtained from the Basra Airport weather station and reanalysis data from the European Centre for Medium-Range Weather Forecasts (ECMWF) and MERRA-2 data to analyze the thermal, humidistic, and dynamic properties of the atmosphere, particularly in the upper atmosphere associated with jet streams. After processing and calculating, the result shows that in 1999, the highest annual frequency of thunderstorms was recorded, with 22 days. The investigation revealed that spring has the highest frequency (56.44%) of thunderstorms. The air stability index (TT and K-indices) was calculated. For the TT index, the category most commonly associated with thundercloud formation is 45-50, accounting for approximately 46.72% of all cases. The k-index category most frequently associated with thundercloud formation is 31-35, which represents about 30.05% of overall cases. The most frequent occurrence of the CAPE coinciding with thunderstorm formation was for values below 300; however, 58.2% of the CAPE frequency fell into two categories, ranging from 300 to 2500 (marginally and moderately convective energy). Pearson correlation analysis reveals that temperature, lifting condensation level (LCL), and equilibrium level (EL) are all moderately to strongly and positively correlated with each other. A strong positive correlation has been found between the convective available potential energy (CAPE) and the equilibrium level and thickness with a p-value < 0.0001 (more reliable).

Keywords: Thunderstorm, Atmospheric stability, K-index, Total Totals index, CAPE, Temperature, Basra Airport.

Introduction

Warm clouds with a high vertical expanse are a defining feature of thunderstorms. The bases of the peaks are typically found close to the highest boundary of the boundary layer, and the peaks can typically reach the tropopause level (Wang, 2013). Thunderstorms are usually accompanied by strong winds, a lot of rain, and occasionally snow, sleet, or hail, while some can produce little to no precipitation. Thunderstorms can create a rain band or line that is referred to as a squall line. Thunderstorms are created when layers of warm, humid air rise in a swift, huge updraft to colder parts of the atmosphere. There, updraft moisture condenses into cumulonimbus clouds, which subsequently generate hail, snow, and precipitation (Krider, 2021; Mondal et al., 2022; Singh & Bhardwaj, 2019). Thunderstorms can develop anywhere in the world, but they are most often in the mid-latitudes, where warm, humid air from the tropical latitudes collides with cooler air from the polar latitudes during the autumnal and springtime instability period

(Bhardwaj et al., 2017; NSSL, 2020). The three essential elements for the formation of thunderstorms are atmospheric instability, sufficient moisture in the lower troposphere, and lifting mechanisms such as convection, frontal lift, and convergence (Arora et al., 2023; Bennett et al., 2006; Kunz et al., 2020; Trapp, 2013).

All thunderstorms (single, multicellular, and supercellular) go through the three stages of development, maturation, and dissipation. A range of several hundred kilometers in size. Depending on the atmosphere, each of these three stages takes an average of thirty minutes. Many potentially hazardous severe weather events develop and are produced during thunderstorms. The primary causes of thunderstorm damage include large hailstones, flash flooding from severe precipitation, and downburst winds (Bhardwaj et al., 2017; NSSL, 2020;Saha et al., 2014; Umakanth et al., 2020). The top of a cumulus cloud may reach deep into the stable stratosphere during a strong thunderstorm. The cumulus clouds will keep expanding and merging with more cells to create a cumulus cloud that reaches even higher into the atmosphere (Ahrens, 2001). Indices like the K-index, Lifted Index, and Convective Available Potential Energy (CAPE) are crucial for meteorologists to assess regional convective potential. They help pinpoint areas with an unstable atmosphere, which is a key condition for thunderstorm development (Humood & Abbas, 2017). When predicting strong convective phenomena, atmospheric instability indices are widely used. However, a variety of factors that prevent the development of the vertical movement of air can have a significant impact on their verifiability. Either upper-air sounding data was used in published studies on the temporal and spatial variability of instability indices (Derubertis, 2006; Madineni et al., 2013). The majority of models struggle to effectively resolve both shallow and deep convection, making forecasting convective weather extremely challenging. Both shallow and deep convection are made possible by shallow convection, which is essential for warming and humidifying the lower atmosphere. Deep convection can spread over the whole troposphere, whereas shallow convection is characterized by its restricted vertical extent. To better understand the processes related to convective weather, it is essential to look at in-situ observations such as radiosonde soundings and vertical profiles of temperature and humidity (Sawaisarje et al., 2025).

Numerous studies have analyzed thunderstorms worldwide in terms of their climatic and geographical distribution. Tyagi (2007) A climatological study of thunderstorms was conducted, encompassing 450 observation stations in India and neighboring countries. Of these, 390 were surface observatories operated by the Indian Meteorological Department, 50 were managed by the Indian Air Force, and the remainder were run by neighboring countries. Al-Khulaifawi & Ioshpa (2023) Thunderstorm activity in Iraq and Turkey is examined in this study, which compares thunderstorm activity from 2010 to 2019 across five meteorological stations in various parts of the two nations. The investigation showed that topography, distance from the sea, and season all had a significant impact on the frequency of thunderstorms in various parts of the world. The data shows that March and April have the highest frequency of thunderstorms in Iraq, with the country's mountainous northern region accounting for 55% of these events. In Turkey, April and May have the highest frequency, with 54% of these happening in southeast Anatolia. There was a lot of thunderstorm activity in the northern and northeastern parts of Iraq, as well as in the southeast of Turkey. The spring season had the highest yearly frequency of thunderstorms. DiGangi et al (2022) To comprehend the features of the thunderstorms in the Marmara Region's airports, a thorough analysis of the storms seen there between 2001 and 2015 was carried out.

On the other hand, further research has focused on dynamic aspects and indicators. Kunz (2007) Utilized 20 distinct stability indices, such as the convective available potential energy (CAPE), K index, and total totals index, to assess Germany's thunderstorm features using radiosonde and SYNOP observations. Rabbani et al (2021) The weather research and forecasting (WRF) model is used to examine the physical and dynamical features of pre-monsoon (March–May) thunderstorms across Bangladesh. Hussain et al (2025) The study was based on data collected between January 26, 2024, and February 9, 2024, from the University of Wyoming data center in the United States. According to the study, the subtropical jet stream affects the 300 hPa layer over Iraq more quickly than the polar jet stream, and there is a significant degree of consistency in the change in temperature and pressure values between the two. That is, the temperature and pressure values rise and fall at the same time, but there isn't a significant time difference over the course of the study.

While some research focused on modern technologies and local studies. Kianusch et al (2025) This study aims to investigate how to improve thunderstorm forecasts by combining numerical weather prediction model data with machine learning. Using the SALAMA ID neural network model, which identifies thunderstorm occurrences in operational forecasts of the ICON-D2-EPS model for the Central European region, a key finding is that the 11-hour forecast achieves the same level of accuracy as the 5-hour forecast. The results showed that machine learning models, such as an example SALAMA ID, can identify predictable thunderstorm patterns for longer timescales compared to raw data from numerical weather prediction models. Zahraa et al (2021) Researchers analyzed thunderstorm dynamics based on total rainfall in Baghdad during 2019. Thunderstorms can be identified in a type of cloud known as cumulonimbus clouds. Data from the European Centre for Medium-Range Weather Forecasts (ECMWF) was used for total daily and monthly rainfall for 2019. The results showed that the highest total rainfall occurred on April 1, 2019, at 15:00. At Baghdad Station, the highest monthly total rainfall for 2019 also occurred in Amadiya, with 392.6782 mm/month at 3:00 a.m. And 391.4047 mm/month at 15:00. As for the stations studied in Iraq, Mosul recorded the highest monthly rainfall, while Rutba recorded the lowest. These days, which experience the highest rainfall, are accompanied by strong thunderstorms.

While these studies are comprehensive, they have not adequately focused on long-term statistical analysis (30 years) to correlate storm frequency in Basra with stability indicators and the effects of regional climate change, which is what your current study will address. For thunderstorms, the study uses reliable non-parametric statistical techniques (such the Mann-Kendall and Mill-Theil-Sen indices). Additionally, this study casts doubt on the CAPE index's dependability in dry conditions worldwide and emphasizes the superior performance of moisture-based indices like K and TT, offering a new predictive framework for comparable semi-arid locations across the globe.

This work aims to analyze and evaluate the characteristics of thunderstorms over Basra Airport stations during the period 1990–2019 and their frequency, temporal distribution, and associated weather factors. It also aims to estimate the atmospheric stability indicators associated with thunderstorm formation using surface weather, ERA-5 reanalysis data, and MERRA-2 data. Furthermore, the work also aims to identify and statistically classify the synoptic systems influencing thunderstorm formation, to improve the understanding of thunderstorm climatic behavior in the region, and to develop future forecasting methods.

2. Materials and Methods

2.1. Study Stations and Data Sources

Iraq is situated between 29˚5′ and 37˚22' N latitude and 38˚45′ and 48˚45' E longitude. Iraq is bordered to the north by Turkey, to the east by Iran, to the south and east by Saudi Arabia, Kuwait, and the Persian Gulf, and to the west by Syria and Jordan. Its geographical diversity includes mountainous regions in the north and northeast, plateau regions at lower altitudes to the south of the mountains, alluvial plains, and western plateaus. The elevation and location of these regions significantly influence the climatic conditions across Iraq. As one moves from south to north, temperatures decrease while rainfall increases (Sultan, 1986; Al-Ansari, 2013). Figure 1 shows the topography of Iraq and the locations of the selected Basra Airport station. In southern Iraq, Basra International Airport is situated about 20 kilometers from the city center to the west of Basra. Basra's climate is categorized as arid-desert climate (Köppen BSh), with extremely hot summers that can reach temperatures of above 50°C and mild to chilly winters with little precipitation. The city's close proximity to the Arabian Gulf contributes to its excessive humidity.

2.1.1. Meteorological Stations Observations

For the years 1990–2019, we used hourly (archived) surface meteorological data from the Iraqi Meteorological Organization on thunderstorms, surface temperature (T), dew point (Td), and air pressure (PPP), particularly for the important times (00:00, 06:00, 12:00, and 18:00). It analyzed the frequency of thunderstorms for the Basra Airport weather station. Basra Airport is located at 30.32° N, 47.39° E, and 3 m above sea level. Basra International Airport is designated by the international air transport association (IATA) code BSR. The airport has one main runway, which is approximately 3400 meters long and 45 meters wide.

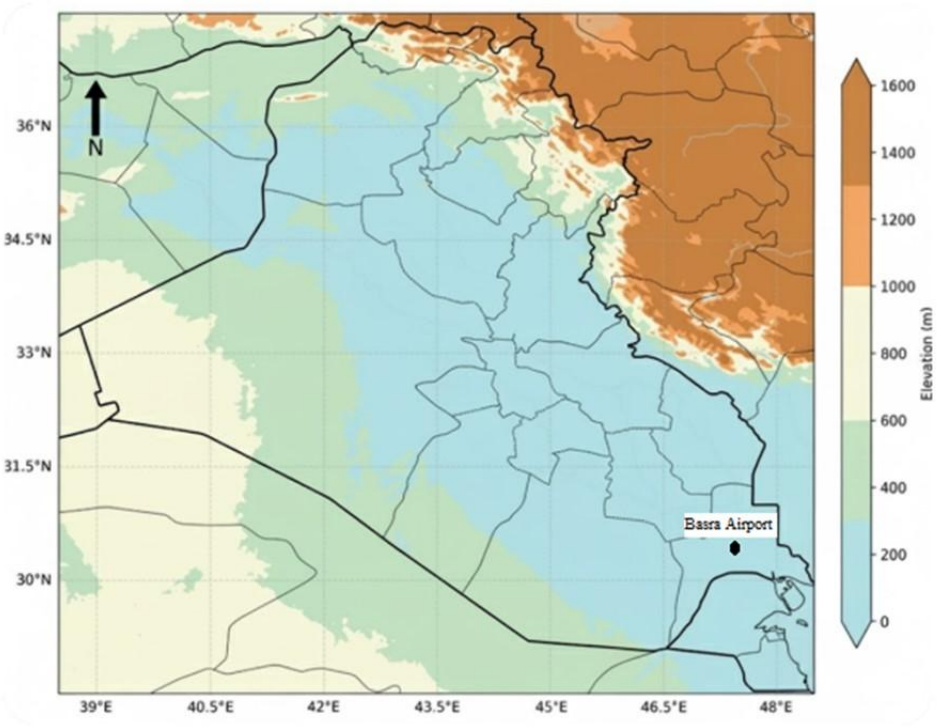


Figure 1. Map of Iraq with the selected station

2.1.2. Reanalysis Data (ERA-5 and MERRA-2)

ERA-5 is the name of the ECMWF Integrated Forecast System's fifth generation. The forecast model incorporates three interconnected elements: ocean waves, land surface, and atmosphere. It provides information on a number of variables at the surface (single level) or upper air level (Hersbach et al., 2023). The utilized data have a temporal resolution of 00, 06, 12, and 18 UTC and a spatial resolution of 0.25° × 0.25° for the atmosphere throughout the 1990–2019 period. The pressure levels are 850, 700, and 500 hPa. The model synopsis is summarized in Table 1.

Table 1: Overview of the ERA-5 driving model.

Characteristics	ERA5
Horizontal coverage	Global
Vertical coverage	1000 hPa to 1 hPa
Outputs	each 6h for upper-air
Horizontal resolution	Reanalysis: 0.25° × 0.25°
Vertical resolution	37 pressure levels
Data assimilation	Yes

MERRA-2 data were mainly used for upper-level synoptic analysis, namely for upper-level divergence at 300 hPa, streamlines, wind speed distribution, and analysis of polar and subtropical jet streams. The ability of MERRA-2 data to accurately depict large-scale dynamic fields sets it apart, especially in areas like the Middle East where there are few upper-level observation stations. It has been used to map wind speed and dynamic structure in the upper atmosphere, giving a more precise description of how the jet stream and lower-level synoptic circumstances cause thunderstorms. In Table 2, the MERRA-2 is summarized.

Table 2: Overview of the MERRA-2.

Attribute	Description

Data type	Modern-Era Retrospective Analysis
Horizontal coverage	Global
Vertical coverage	Surface to 0.01 hPa
Primary pressure level used	300 hPa
Horizontal resolution	0.5° × 0.625°
Temporal resolution	3-hourly
Main application in this study	Jet stream analysis, wind speed, streamlines, Weather diagnosis
Data provider	NASA - Global Modeling and Assimilation Office (GMAO)

2.2 The Calculations of Some Indices and Parameters

2.2.1. K – Index

The K-index is a thunderstorm potential indicator that is based on the amount and vertical extension of low-level moisture in the atmosphere as well as the vertical temperature lapse rate. Table 3 shows atmospheric conditions by K-index values. Using temperature (T) and relative humidity (RH), the dew point (Td) and dew point depression (DD=T-Td) were determined. This indicator rises with increasing moisture at 850 hPa, rising relative humidity at 700 hPa, and decreasing static stability between 850 and 500 hPa. The K-index was then determined using the following formulas (Buck, 1981; George, 1960; Viceto et al., 2017):

$$K = T\,(850mb) + Td\,(850mb) - T\,(500mb) - DD\,(700mb) \quad (1)$$

2.2.2. Total Totals Index

Using temperature and dew point data at 500 hPa and 850 hPa levels. This formula is used to calculate it (Miller, 1972; Ye et al., 1998; U.S, 1990):

$$TT = T850mb + Td850mb - 2(T500mb) \quad (2)$$

Information about the state of the atmosphere according to the value Total Totals index ranges of this parameter, as shown in Table 3.

2.2.3. Convective Available Potential Energy (CAPE)

Its foundation is the integration of the atmosphere's vertical profile. Smaller values of this parameter show that the atmosphere is stable. While larger values show that the atmosphere is unstable, As the temperature differential between the warmer parcel and the cooler environment develops, strong convection necessitates a larger CAPE and updraft acceleration (Lucas et al., 1994; Miller et al., 1972; Showalter, 1953). It is calculated by the following formula:

$$CAPE = g * \int_{LFC}^{EL} (Tp - Te) * dz/Te \quad (3)$$

In this formula:

LFC: is the free convection level, expressed in hPa or mb;
LE: level of equilibrium, expressed in hPa or mb;
Te: is the surrounding temperature in degrees Celsius;
Tc: is the temperature of the cloud parcel in degrees Celsius;
g: is the gravitational acceleration, expressed in m/s^2.
dz: is the layer's thickness between the LFC and EL levels, expressed in m or km.

Information about the state of the atmosphere according to the value (CAPE) ranges of this parameter, as shown in Table 3. Additionally, the data (CAPE) comes from the Physical Sciences Laboratory's (NOAA) Vertical

Profiles of Reanalysis Datasets (https://psl.noaa.gov/data/atmoswrit/profile/). For almost every country on the earth, they contain a Skew-T diagram, a vertical profile, and climatic parameters.

Table 3: Atmospheric stability is based on the CAPE value (NWS, 2022; Ye et al., 1998).

Indices/parameter	measurement unit	Value (Indices/parameter)	Thunderstorm Probability (Types)
K-index	ºC	K below 20	Thunderstorms unlikely or none
		K between 20 to 25	Isolated thunderstorms
		K between 26 to 30	Widely scattered thunderstorms with rain or severe weather
		K between 31 to 35	Scattered thunderstorms with heavy rain
		K above 35	Numerous thunderstorms with very heavy rain and hail
Total Totals index	ºC	TT below 45	Thunderstorm unlikely
		TT between 45 to 50	Thunderstorms possible
		TT between 51 to 52	Isolated severe thunderstorms
		TT between 53 to 56	Scattered severe thunderstorms
		TT above 56	Severe thunderstorms most likely; tornado
Convective Available Potential Energy (CAPE)	J/Kg	CAPE below 300	Stable atmosphere
		CAPE 300 to 999	Marginally unstable atmosphere (Light to moderate rain)
		CAPE 1000 to 2499	Moderately unstable atmosphere (Heavy rain with small hail)
		CAPE 2500 to 3500	Very unstable atmosphere (Very heavy rain with large hailstones)
		CAPE >3500	Extremely unstable atmosphere (Tornado)

Using the LCL values, the cloud base height is roughly estimated, which is obtained using surface temperature and dew point temperature information (the air temperature equals to the dew point temperature at this altitude). In order to calculate convective available potential energy (CAPE) and convective inhibition (CIN) and analyze thunderstorm potential and severity across any region, the LCL values are crucial. To determine the direct relationship with the total water vapor content, cloud height variability, seasonal and regional variability, etc., the LCL values can be employed as CBH (Craven et al., 2002b; Xu et al., 2019). While EL, the height at which the temperature of the flowing air parcel equals the ambient temperature, is known as the equilibrium level, the EL values can be employed as CTH (Cinaroglu & Unutulmaz, 2018). And calculating the depth of the cloud, or vertical thickness, by the disparity between the cloud's base and summit heights is known as this parameter (Shmeter, 1972).

This research plan describes (Figure 2) a methodology for analyzing climate data to study and classify thunderstorm events using an integrated approach. It is based on, first, the primary data used, which are from the Basra Airport meteorological station and ERA-5 and MERRA-2 data. This model integrates vast amounts of historical observations (from satellites, ground stations, and balloons) with advanced numerical models to provide a

comprehensive picture of past atmospheric conditions. Second, the process includes data collection and preprocessing, followed by climate analysis and calculation of key atmospheric instability indices and parameters. These help assess the probability of convective events. Third, atmospheric maps are analyzed to identify the systems influencing the weather, and then the events are classified. Finally, linear and nonlinear correlation testing is used to determine the relationships between the various parameters.

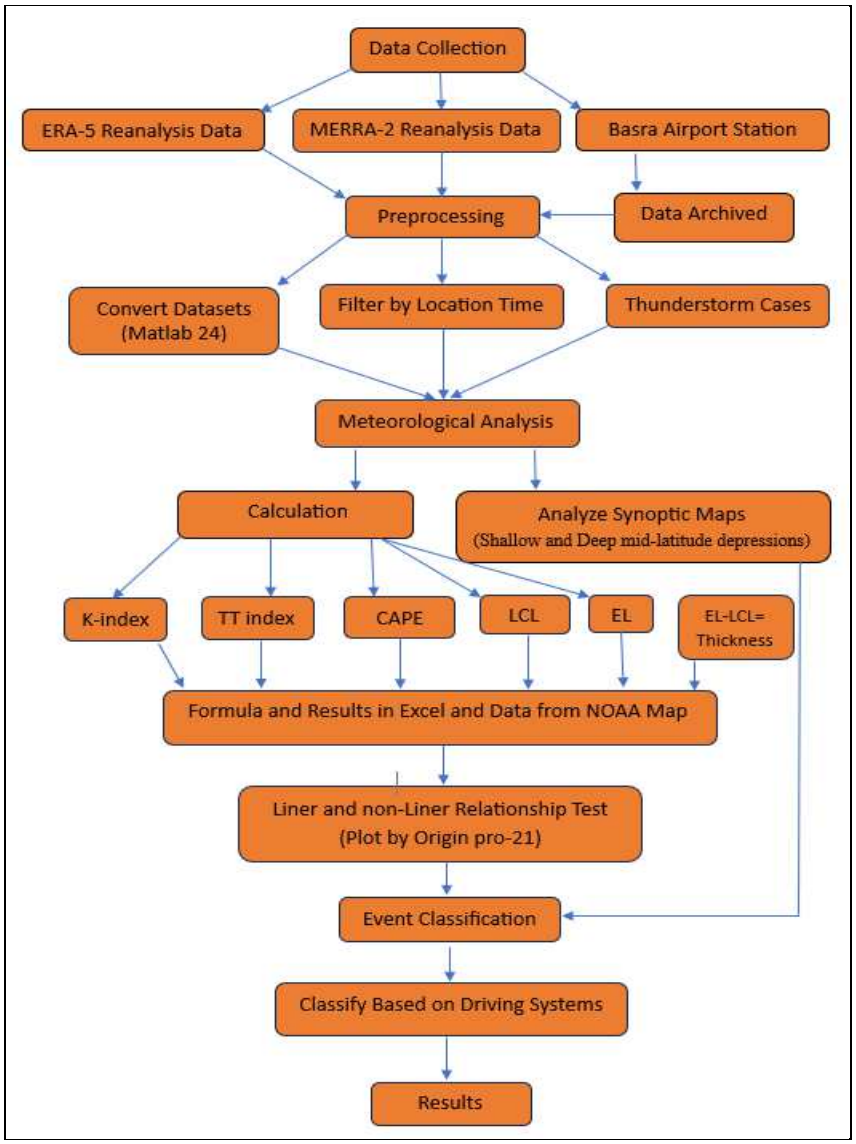


Figure 2. Work Methodology Flowchart

3. Results and Discussion

3.1. Thunderstorm Frequency on a Monthly and Annual

Figure 3 shows the time distribution of the annual frequency of thunderstorms at the Basra Airport station for the period from 1990 to 2019. There is no discernible long-term pattern of an increase or decrease in the number of thunderstorms, as the figure illustrates. The dynamic and thermal conditions of the area are directly linked to the shifting nature of the weather parameters that affect thunderstorm formation, which is reflected in this fluctuation. The

highest frequency of thunderstorms was recorded in 1999, with around 22 storms, indicating exceptional thunderstorm activity that may be related to unusual weather conditions such as increased atmospheric instability or an increase in (CAPE) during that season. In contrast, the lowest frequency was observed in 2005, 2009, and 2012, with the number of storms not exceeding approximately three storms, which may reflect relative atmospheric stability and a decrease in atmospheric humidity or a weakness in the development of cumulonimbus clouds. Additionally, there was a noticeable rise in thunderstorm activity during the 1990s (1997–1999), which may have coincided with times when regional climate oscillations like the North Atlantic Oscillation (NAO) or the El Niño phenomenon (ENSO) were prominent (NOAA, 2016). Which affect rainfall patterns and atmospheric instability in the Middle East regions. An analysis of the number of Mediterranean storms that make it to Iraq reveals no discernible difference between the number of cyclones that occur during the NAO's positive and negative phases. The cyclones' varying intensities do exist, though (Khidher & Pilesjö, 2014). This implies that precipitation does not always accompany thunderstorms; rather, it relies on the kind of cloud or the cloud types connected to the low-pressure system as it moves across the area. In contrast, there was no discernible rise in thunderstorm activity during the 2000s. Over the previous thirty years, there has been no discernible linear trend in the climatic record for thunderstorms at Basra Airport station. This implies that short- to medium-term climate fluctuations rather than long-term climate change are more responsible for the change in storm frequency. Future trends in thunderstorm activity in the area might be clarified, though, by continuing to collect and analyze thunderstorm data over longer time periods and connecting them to elements like surface humidity, lower air temperatures, and atmospheric pressure distribution.

Statistical analysis using the Mann-Kendall test showed a statistically significant decrease in the number of annual thunderstorm days at Basra Airport during the period 1990–2019 ($Z = -2.71$, $P < 0.0067$). This indicates that the observed change in the graph is real and statistically significant, and not merely coincidental. The Theil-Sen slope estimator indicated a decrease of -0.312 days per year. This means that the storm frequency decreased by 9.3 days over the past 30 years.

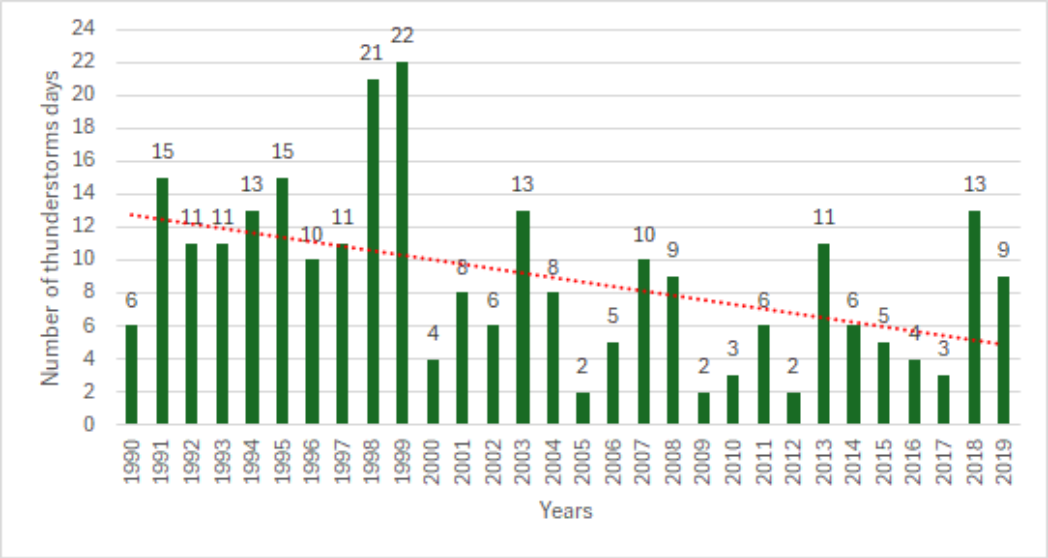


Figure 3. Annual distribution of thunderstorms at Basra Airport station for the period (1990-2019)

Figure 4 shows the monthly distribution of thunderstorm frequency recorded at Basra Airport station during the period from 1990 to 2019. According to analysis, the region's thunderstorm activity exhibits a clear seasonality, with the majority of storms occurring in spring and autumn and peaking in March and April. The highest frequency of thunderstorms was recorded in April, with the number of cases exceeding 75 storms, this accounts for 29.92% of all frequencies (averaging 2.5 events per month) during the study period, followed by March with more than 40 storms,

(averaging 1.5 events per month), reflecting an increase in atmospheric instability rates during the spring months as a result of the intersection of cold air masses coming from the upper latitudes with a warm, moist air masses from the lower latitudes. These conditions lead to enhanced convection and the formation of cumulonimbus clouds, which are responsible for thunderstorms. With 149 events, approximately five thunderstorms each season, spring is the season with the highest frequency of thunderstorms, accounting for 56.44% of all frequencies.

However, during the summer, no thunderstorms were noted or seen. As for the autumn season, September is the least active month, with the number of recorded storms not exceeding approximately 3. This is attributed to the dominance of subtropical high-pressure systems during the summer months, which stabilize the atmosphere and prevent the development of cumulonimbus clouds. Due to the return of low-pressure systems that move through the area and the start of the thermal influence's reduction, moderate-rate thunderstorm activity is observed in October and November with 24 (averaging 0.8) and 35 (averaging 1.2) thunderstorm events, respectively. With 62 recorded thunderstorms, approximately two each season, autumn is the second most common season, accounting for 23.49% of all frequencies.

During winter, thunderstorms occur at below-moderate rates, with 15 to 21 events per month (averaging 0.5-0.7 events). There are 53 recorded thunderstorms throughout the winter, which equates to 1.8 thunderstorms each season, accounting for 20.07% of all frequencies. This is because cold fronts from mid-latitude low-pressure systems provide little instability. According to this trend, Basra's thunderstorm activity is mostly determined by seasonal dynamics and thermal parameters. Spring emerges as the most favorable period for storm occurrence due to elevated surface temperatures, increased relative humidity, and enhanced convective processes. The monthly distribution of thunderstorms aligns with the arid and desert climate of the Basra region, where transitional seasons experience more frequent weather disturbances than the more stable summer and winter periods.

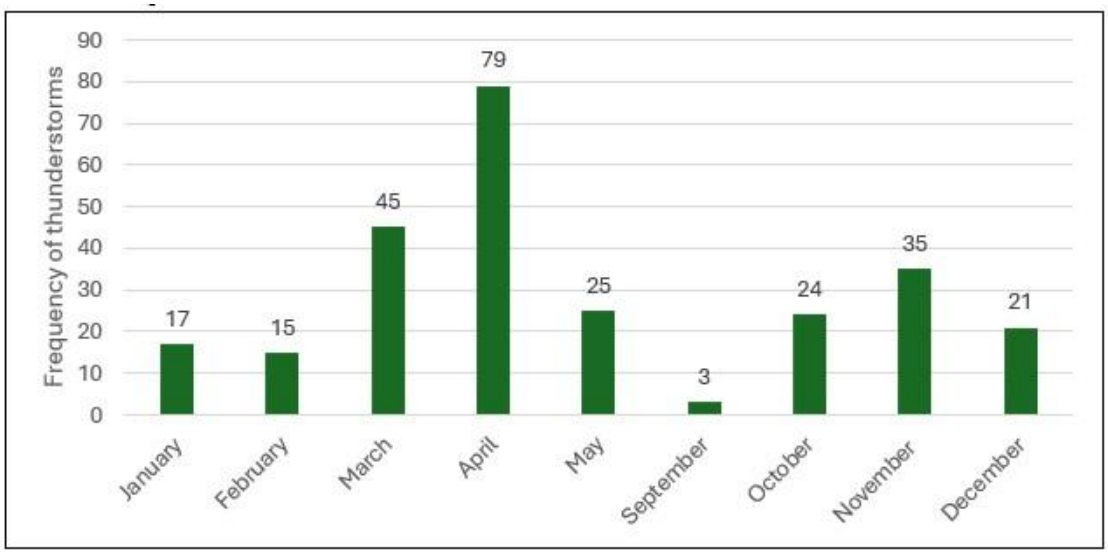


Figure 4. Monthly distribution of thunderstorms at Basra Airport station for the period 1990-2019

Figure 5 shows the relative distribution of synoptic system types associated with thunderstorm occurrence at Basra Airport station during the period from 1990 to 2019 and for six months of the year (March, April, May, September, October, and November). The results show that shallow mid-latitude depressions accounted for the largest proportion of impactful cases at 54.98% of the total depressions, while deep mid-latitude depressions accounted for 45.02%. This distribution shows that the majority of thunderstorms in the Basra region are produced by somewhat shallow atmospheric systems, which reflects the region's transitional climate. In line with regional climate change indicators that indicate rising temperatures and decreasing atmospheric humidity in Iraq, the continued dominance of shallow depressions by a small percentage over the past three decades may reflect a gradual shift, similar to climatic influences, towards more prominent local warm patterns. This shift highlights the necessity of a long-term dynamic

investigation of the weather systems influencing the region, as it is important for improving thunderstorm forecasting systems and reducing their impact on agricultural and urban activities in Basra Governorate and neighboring areas.

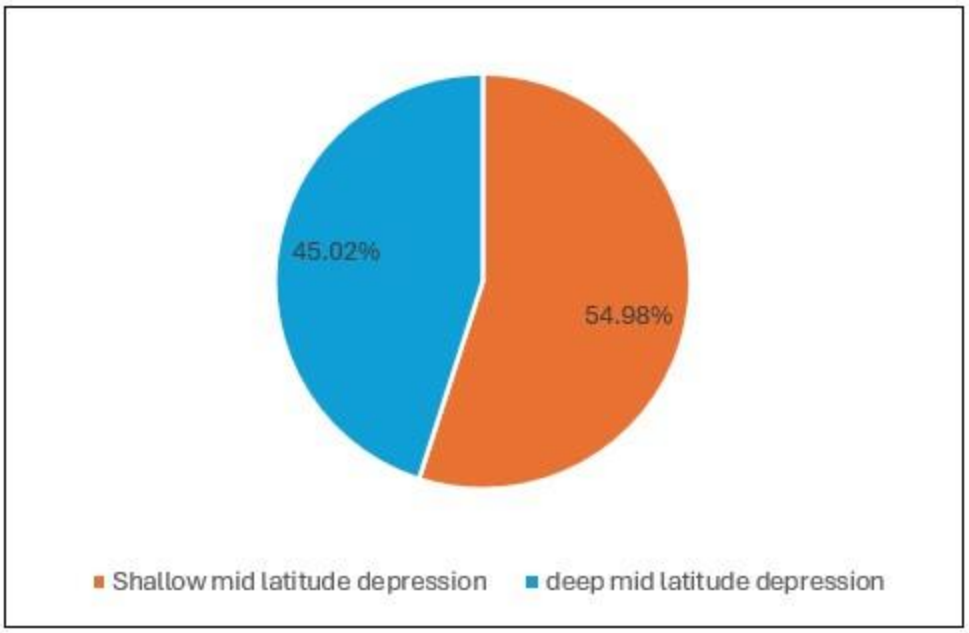


Figure 5. The relative distribution of Shallow and Deep mid-latitude depressions at Basra Airport station for the period 1990-2019

Figure 6 shows the frequency distribution of the thunderstorm (K-Index) for the period between 1990 and 2019 (366 events). The histogram shows a fluctuation in the frequency of index values, indicating shifts in the characteristics of atmospheric instability over the previous thirty years. According to the results, 30.05% of the observations fall into the category between 31 and 35. The category 26–30 follows at 28.14%. These values express medium to high levels of thermal and moisture instability. They are often associated with the formation of cumulus clouds and local thunderstorms. The highest frequency ratios, which fall between 26 and 35, show that the study period's atmospheric conditions were ideal for moderate to intense convection. This corresponds with the climate of the study's area, which is frequently impacted by heat waves and times of high relative humidity in the lower layers. These conditions create vertical instability. In contrast, categories with low values ($K < 20$), amounting to 17.49%, represent cases of atmospheric stability. These situations are linked to upper-level cooling or dominant dry air masses, which restrict convection and lessen cumulus cloud formation. Very high values ($K \geq 40$) did not exceed 4.92% and reflect rare cases of extreme instability. This is frequently associated with exceptionally humid tropical activity or the passage of deep low-pressure systems. The results indicate that the K index at the study station has high values. This means the probability of thunderstorms is relatively frequent but mostly not severe. In short-term weather forecasting, this pattern is a crucial indicator. This indicator's distribution can be used to determine the likelihood and intensity of local meteorological events. Additionally, changes in index value distribution over time can enhance understanding of the relationship between thermal and humidity activity and regional climate change in recent decades. The K index is based on the moisture content in the lower layers of the atmosphere, making it more suitable for diagnosing short-term local thunderstorms (forecast TSs that happen when there are no frontal or cyclonic influences and there is minimal wind).

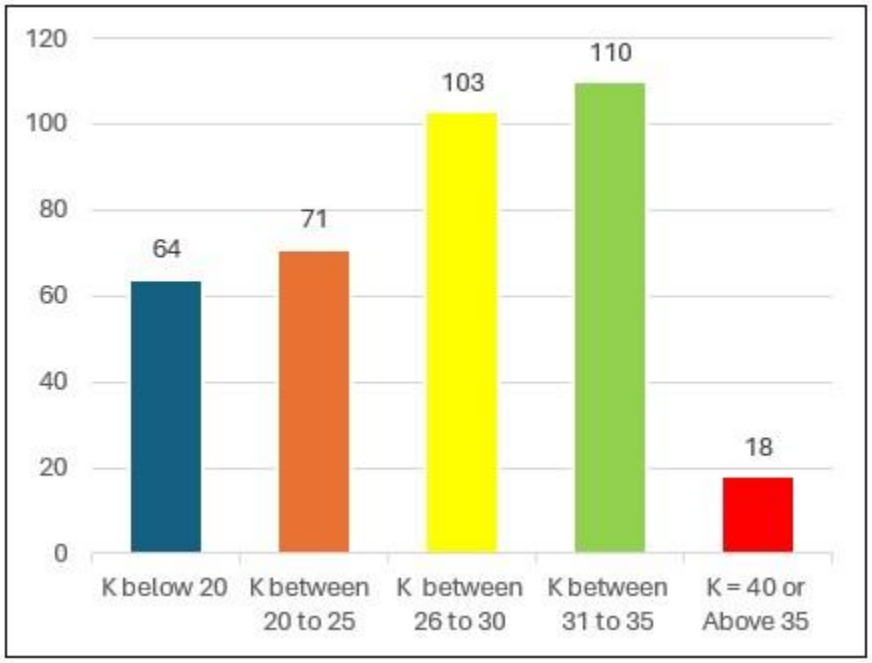


Figure 6. K-index frequency of thunderstorms at Basra Airport station for the period (1990-2019)

Figure 7 shows the frequency distribution of the thunderstorm (Total Totals index) for the period between 1990 and 2019, indicating that the category between (45–50) is the most frequent at (46.72%), followed by category (51–52) at (23.77%). As TT values in this range are typically linked to an adequate thermal and humid environment for the formation of cumulonimbus clouds and the occurrence of local, limited-intensity thunderstorms, these values show an increase of moderate atmospheric instability in the area. As for the low categories (TT < 45) and (53–56), they amounted to (13.93%) for both categories, while the very high values (TT ≥ 57), which amounted to (1.64%), reflect rare cases of extreme instability, often associated with strong thermal lifting processes or the passage of severe atmospheric depressions. The TT index is a useful tool for detecting thunderstorm activity and estimating the possibility of atmospheric disturbances in the area because, overall, its distribution demonstrates that the majority of the investigated periods were marked by moderately unstable circumstances.

The results of the frequency distribution of both the K and TT indices for the period (1990–2019) showed that both clearly reflect the thermal and humid nature of the atmospheric layers in the study area, but there is a difference in the intensity of the response and the accuracy of representing instability conditions. Both indices correctly depict the dominance of moderate-high instability in the local climate, with K values concentrated between 26 and 35 (58.20%) and TT values concentrated between 45 and 52 (70.49%). However, the K index is more closely related to the moisture content in the lower layers of the atmosphere and, therefore, more sensitive to changes in relative humidity and more effective in predicting short-lived local storms. The TT index, however, relies more heavily on the vertical temperature gradient between the 850 and 500 hPa layers, making it better able to represent large-scale disturbances and deep thunderstorms. Therefore, it is recommended to use both indices together for a more accurate assessment of atmospheric instability levels and to predict thunderstorm activity in the region. The results of the analysis of the K-Index and Total Totals Index indicate that the atmospheric climate over Basra Airport during the period (1990–2019) was characterized by a high frequency of moderate-high instability, with a scarcity of severe cases, which reflects a transitional nature of the atmosphere between near-permanent stability during periods of drought and limited instability during the transitional and spring seasons. This distribution supports the theory that episodes of atmospheric disturbance have grown more frequent but less intense due to a redistribution of thermal energy and moisture characteristics in the lower layers of the atmosphere caused by regional climate change. Long-

term monitoring of these two indicators would provide a scientific basis for developing early warning systems and improving the accuracy of thunderstorm forecasts in the region.

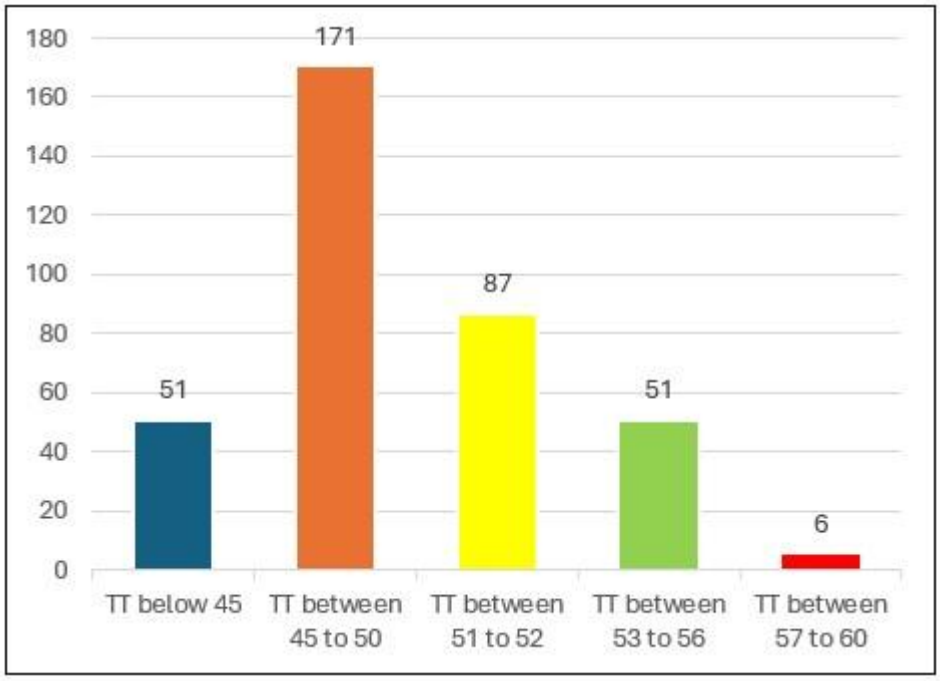


Figure 7. Total Totals index frequency of thunderstorms at Basra Airport station for the period (1990-2019)

Figure 8 illustrates the frequency distribution of the thunderstorm (available convective thermal energy coefficient (CAPE)) across different categories for the period from 1990 to 2019, providing a fundamental basis for understanding atmospheric stability and the potential for thunderstorm development in the study area. With just a slight increase in the likelihood of severe storms, the data show a dominance of very stable or weak convective weather. According to the data, the following categories comprise the CAPE parameter frequencies:

• CAPE below 300: This is the most prevalent category, accounting for 38.80% of all observations. When there is not enough upward buoyancy to sustain the formation of powerful thunderstorms, the range of extremely low values denotes stable or extremely stable atmospheric conditions. This results in a notable lack of convection or weakening, supporting the existence of either insufficient heat in the surface layers or a strong convective inhibition (CIN) layer.

• CAPE category 300 to 999: This category represents the third most common category, at 26.78%. These values, which are normally classified as marginally convective energy, show the development of mild thunderstorms or cumulonimbus clouds but are not strong enough to produce violent weather occurrences. The region's atmospheric cover was, for the most part (during the study period), either stable or with a low sensitivity to convection, as confirmed by the sum of these two categories, which is roughly 65.57%.

• CAPE 1000 to 2500 category: This category represents a frequency of 31.42%. These values are considered medium to high, which indicates the possibility of strong thunderstorms accompanied by heavy rainfall and possibly small hail. The majority of meteorological phenomena in the area that might be classified as "storms" fall into this category. The frequency decreases sharply as the CAPE value increases, reflecting the rarity of extreme instability conditions.

• CAPE category 2500 to 3500: Represents a small percentage of 2.19%, which is very low. This range shows highly unstable atmospheric conditions, which increase the chance of severe thunderstorms. Higher values indicate stronger convective energy and a greater risk of severe weather, including supercells.

• CAPE category > 3500: This category is the least common, representing only 0.82%. These high values indicate extremely rare and violent weather phenomena, including large hailstones, tornadoes, heavy rain, and intense lightning (electrical activity is very high), confirming that these events are exceptional in the region.

These results can be used as a "ground truth" to evaluate the performance of regional climate models in simulating atmospheric stability conditions. The distribution provides the statistical basis for risk assessment; most days of the year require low warnings (within the range of CAPE < 1000), while severe storm days (CAPE > 2500) are rare and warrant a special early warning system. This distribution can also be compared with the expected changes under global warming scenarios to estimate how much the frequency of strong storms will increase or decrease. The distribution suggests the need for future research to focus on identifying the dynamic and thermodynamic factors (such as wind shear and moisture distribution) that contribute to rare cases of extreme instability, rather than focusing solely on CAPE parameter averages. Even in conditions with low CAPE, strong vertical wind shear can encourage the development of thunderstorm occurrences. Despite their low energy, wind shear can enable thunderstorm occurrences to form and persist for a long period by sustaining updrafts (Weisman & Klemp, 1982).

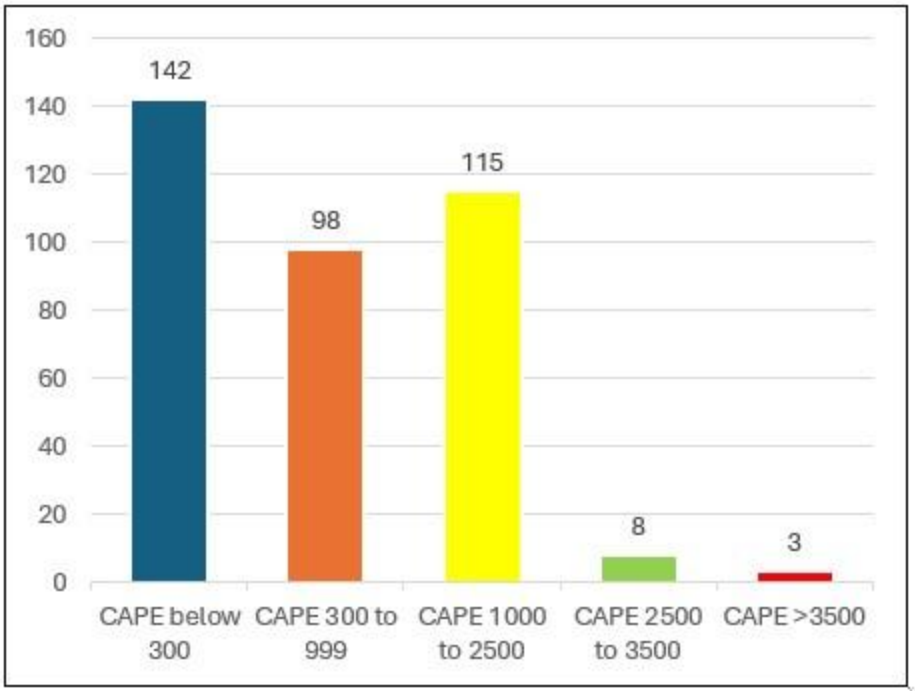


Figure 8. CAPE parameter frequency of thunderstorms at Basra Airport station for the period (1990-2019)

Based on the results, the TT index is considered one of the best indicators for predicting thunderstorms. Over 30 years, as TT values ranging between 45 and 50 indicate a high probability of thunderstorms occurring, the probability increases with the increasing value of the index. The data shows that 46.72% of storms in Basra fall within this range, making it a reliable indicator. In contrast, the CAPE is less accurate, with 38.80% of thunderstorms falling within a range below 300 (atmospheric stability). Through skew-T analysis, it was found that the majority of convection energy falls within this level (from 900 or 850 to 700 or 650 hPa). Forecasts, however, frequently indicate

that indicators based on available convective potential energy, such as CAPE, would be better at forecasting thunderstorms. Yet, data analysis has shown that the opposite is true, and it is better at forecasting non-thunderstorms.

Analyzing the graphs above (6-8), we observed a slight, gradual increase in the average values of the indices over time (1990-2019).

Table 4 shows a monotonic trend analysis using the Mann-Kendall test and the Theil-Sen estimator for all convection coefficients (1990–2019). The results indicate that the average dynamic indices (CAPE, K, TT) above Basra Airport have not exhibited a monotonic trend (no upward or downward movement) over the past 30 years. This suggests that the environmental stress is highly inter-annual and lacks a consistent linear trend. There are no statistically significant long-term trends for CAPE (p= 0.83), Ki (p= 0.41), or TTi (p= 0.14). This indicates that the environmental potential for thunderstorms in Baghdad is characterized by sharp annual fluctuations (depending on the load-lift mechanism, dynamic changes, and relative humidity to a large extent due to Basra's dry climate) rather than a stable climatic shift, which maintains a quasi-stable potential for convection initiation over three decades.

Table 4: Statistical analysis using (Mann-Kendall test and Theil-Sen slope for indices (1990-2019).

Index	Z	p-value	Theil-Sen Slope	Trend
CAPE Average	0.21	0.83	0.74	No Trend
K-index Average	0.82	0.41	0.04	No Trend
Total Totals Average	1.46	0.14	0.06	No Trend

3.2. Efficient Stability Indices in Severe Cases

We select four extreme scenarios to comprehend the behavior of the K, Total Totals indices, and CAPE.

Case 1: April 1995 (period of most intense thunderstorm events)

- The CAPE showed a significant increase and exceeded 1400, indicating a high probability of moderate thunderstorm events.
- The K index showed an increasing trend and surpassed 33 during the days of the greatest number of severe thunderstorm events.
- The Total Totals index (TT) showed a rapid rise over 55, which was accompanied by a sharp rise in the number of thunderstorm activities in April, with 12 events.

Case 2: March 1999 (early spring thunderstorm event period)

- The CAPE showed a significant increase and exceeded 1400, indicating a high probability of moderate thunderstorm events.
- The K index showed an increasing trend and surpassed 32 during the days when there were scattered thunderstorm events.
- The total totals index (TT) also showed a considerable increase exceeding 55, indicating a high probability of extreme thunderstorm events. That correlates with the peak of thunderstorm activity in March, which had 7 events.

Case 3: April 2003 (Mid-Spring thunderstorm event period)

- The CAPE showed a significant increase and exceeded 3800, indicating a high probability of extreme thunderstorm events.
- The K index showed an increasing trend and surpassed 36 during the days when there were risky thunderstorm events. That correlates with the peak of thunderstorm activity in April, which had 7 events.
- The Total Totals index (TT) observed a large increase over 50, indicating a probability of severe thunderstorm events.

Case 4: April 2007 (Mid-Spring thunderstorm event period)

- The CAPE showed a significant increase and exceeded 2000, indicating a high probability of moderate thunderstorm events.
- The K index showed an increasing trend and surpassed 34 during the days when there were severe thunderstorm events. That correlates with the peak of thunderstorm activity in April, which had 7 events.
- The Total Totals index (TT) observed a large increase over 57, indicating a high-risk probability of scattered severe thunderstorm events.

3.3. Analysis and Evaluation of the Correlation Coefficient Between Temperature, LCL, EL, Thickness, and Atmospheric Stability Parameter (CAPE)

The linear relationship in Figure 9 between potential available convective energy (CAPE) and temperature (T) shows a moderate positive correlation ($r = 0.5$), indicating that as temperature (T) increases, CAPE increases as well, and vice versa. Elevated surface air temperature is a major factor in increasing atmospheric instability, thereby increasing available latent convective energy (CAPE), which fuels and develops thunderstorms. The wide dispersion of data points around the red regression line indicates that temperature is an influential factor, but not the only one. Other factors (such as humidity, wind, and vertical changes in the atmosphere) also play an important role in determining the CAPE value. This is because surface heating raises the temperature of air parcels near the surface, which leads to a decrease in their density and gives them the necessary acceleration to begin the process of floating within the atmosphere; thus, they rise to higher layers, where they can release their latent energy in the form of effective convection. The empirical equation for linear regression ($CAPE = -655.2 + 61.4*T$) shows that (every 1°C increase in temperature theoretically leads to an increase in convection energy of 61.4 J/kg) with an expected value of around 4000 J/kg at higher temperatures, which indicates that surface temperature is the primary factor in initiating and sustaining thermal instability, as it directly controls the amount of energy available for convection.

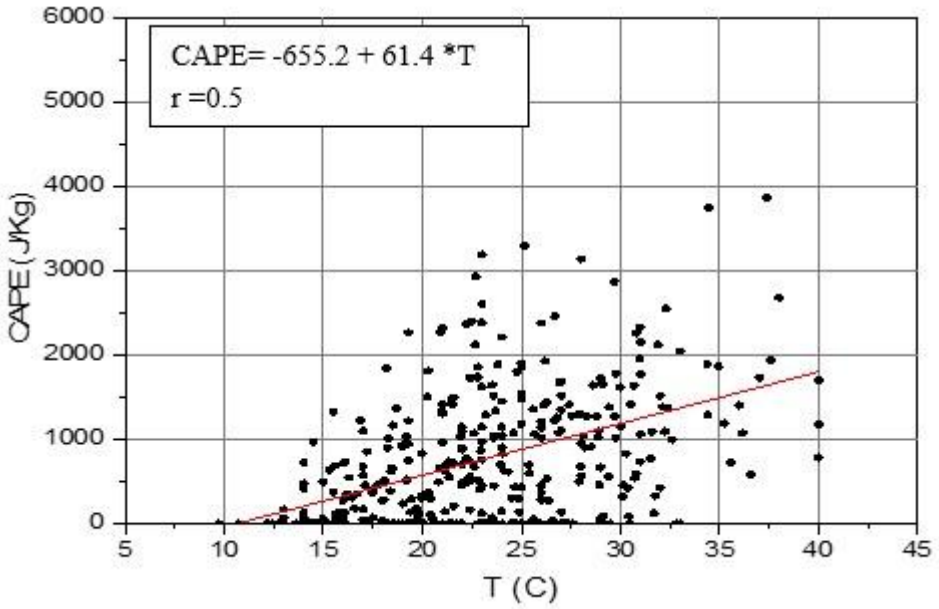


Figure 9. The correlation coefficient between Temperature and CAPE

The results show a relatively strong positive relationship between surface temperature (T) and the lifting condensation level (LCL), with a correlation coefficient of r = 0.7 in Figure 10, indicating that a rise in surface temperature leads to a rise in the level of condensation in the atmosphere. The empirical equation for linear regression (LCL = -1508.3 + 114*T) expresses this relationship, indicating that every 1°C increase in surface temperature corresponds to an increase of approximately 114 meters in the height of the condensation level. This behavior is attributed to the fact that a higher surface temperature increases the air's ability to hold water vapor, leading to a decrease in relative humidity and a move away from a state of saturation. As a result, the air needs to rise to higher levels in order to cool and reach the dew point, that is, the point at which actual condensation begins. This explains the marked increase in LCL values with rising temperature. As can be seen from the figure, the dispersion of data points around the regression line indicates that the relationship is also influenced by other factors such as the actual amount of water vapor in the surface layer, daily variations in terrestrial heating and radiation, as well as local surface characteristics (soil moisture, vegetation cover). However, the high correlation strength (r = 0.7) confirms that surface temperature remains a key and direct factor in determining the height of the condensation level. In general, this relationship reflects that hot, dry conditions lead to a higher condensation level (LCL), which reduces the likelihood of low cloud formation, while cold, humid conditions lower the LCL and increase the chances of vapor condensation and cumulus cloud formation.

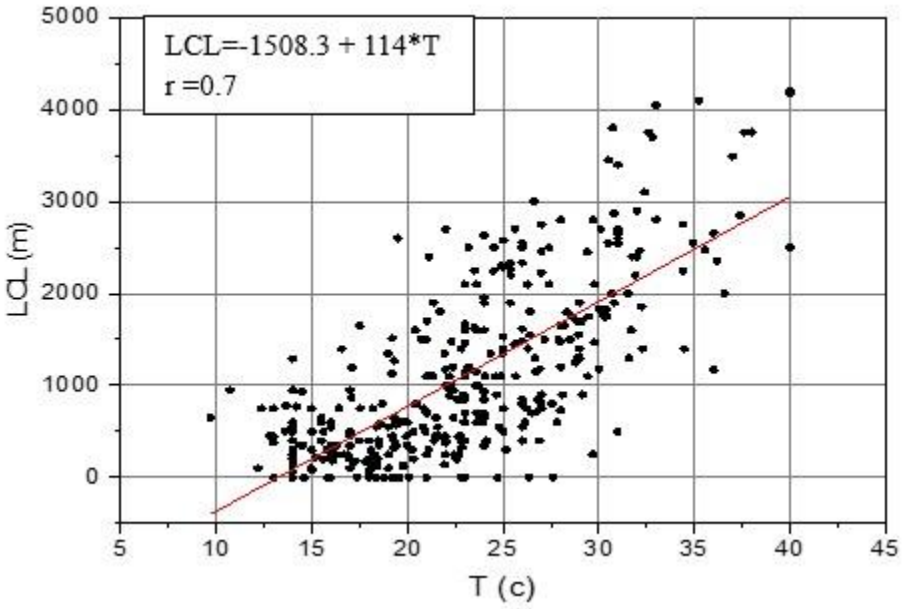


Figure 10. The correlation coefficient between Temperature and LCL

The relationship between temperature and equilibrium level, as shown in Figure 11, was analyzed using a non-linear regression model (ExpGro2). The data show a clear positive correlation between them ($R^2 = 0.5$). That is, the rise in temperature is associated with an increase in the height of the equilibrium level in the atmosphere, which is consistent with the thermodynamic principles that link the heating of the lower layers (high temperatures) with the rise in equilibrium levels. Despite the clear positive trend, the graph points show a large dispersion around the red regression line. This dispersion indicates that the strength of the correlation is moderate and that temperature, although an important factor, does not alone explain the entire variance in the equilibrium level, indicating the intervention of other atmospheric factors such as (humidity content, wind shear, and vertical changes in the atmosphere) in predictive models to increase the accuracy of explaining the variance in the equilibrium level. This is because surface heating raises the temperature of air parcels near the surface, which leads to a decrease in their density and gives them the necessary acceleration to begin the process of floating within the atmosphere, and thus they rise to higher layers, where they can release their latent energy in the form of effective convection. This indicates that surface temperature is the primary factor in the initiation and maintenance of thermal instability.

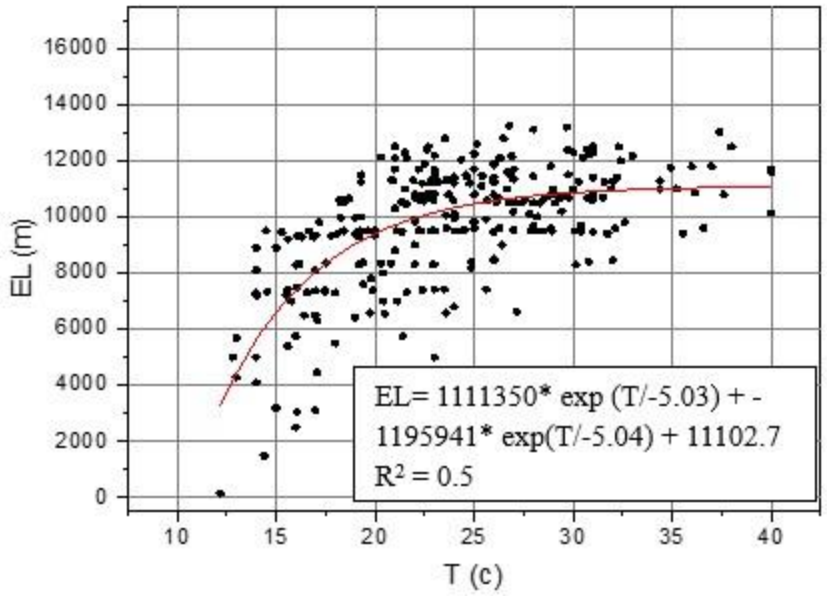


Figure 11. The correlation coefficient between Temperature and EL

From Figure 12, the data indicate a strong positive correlation (R^2 = 0.94) between the potential available convective energy (CAPE) and the equilibrium level (EL). This relationship was plotted using an exponential growth model (ExpGro2). As the CAPE value increases, the equilibrium level (EL) also increases. The increase in the equilibrium level is sharp and rapid at low and medium CAPE values (less than about 2000 J/kg), then the curve begins to saturate or flatten at high CAPE values. This indicates that the effect of increasing CAPE on raising the equilibrium level becomes less pronounced after a certain limit, and the equilibrium level approaches an approximate maximum value. Although there are scattered points with high dispersion, especially at CAPE values exceeding 2000 J/kg. This analysis confirms the important role of CAPE as a catalyst for convection and its direct relationship to the maximum height of deep convective clouds.

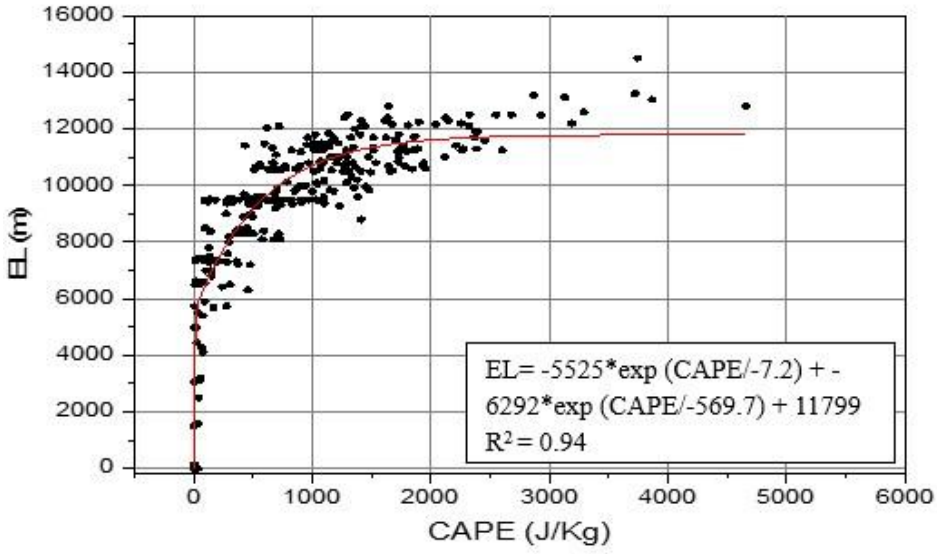


Figure 12. The correlation coefficient between CAPE and EL

From Figure 13, the data clearly indicate a strong positive and non-linear correlation ($R^2 = 0.9$) between the potential available convection energy (CAPE) and thickness. Using an exponential model (ExpGro2), the layer thickness increases as the CAPE value increases. This increase is more pronounced and rapid at lower CAPE values (below approximately 1000 J/kg). As CAPE continues to increase, the curve begins to flatten (saturate), indicating that the effect of subsequent CAPE increases on layer thickness becomes less significant at higher values. Despite the strong correlation, a noticeable dispersion is observed in the graphs, particularly at high CAPE values. This dispersion suggests that CAPE is not the sole factor influencing layer thickness and that other atmospheric factors play a significant role in the remaining variation. This indicates that surface temperature is the primary factor in initiating and sustaining thermal and atmospheric instability.

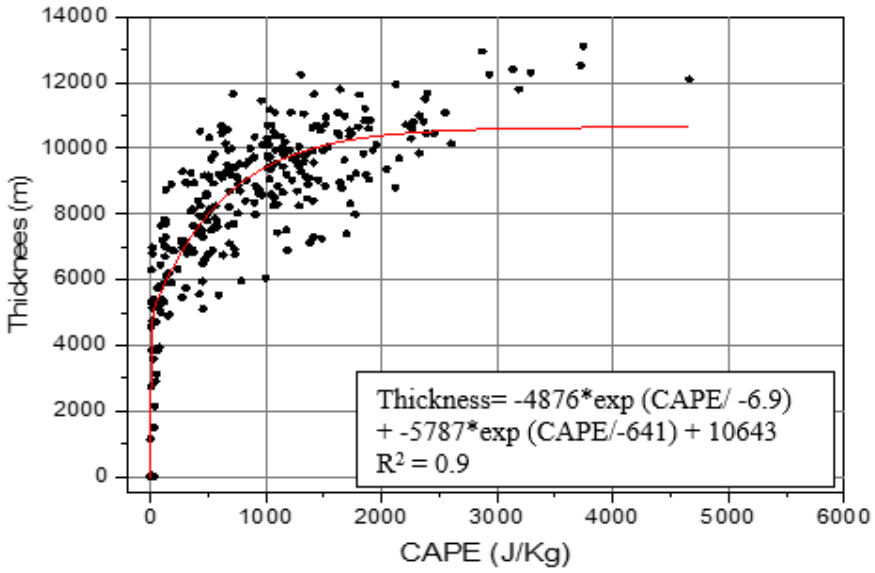


Figure 13. The correlation coefficient between CAPE and Thickness

Table 5 shows statistical relationships using linear and non-linear/exponential growth (ExpGro2) models. Temperature (T) had medium to strong, significant linear correlations with CAPE and thermal lift (LCL) (R = 0.5–0.7, P-values = <0.0001–<0.0006). Available convection energy (CAPE) showed a strong exponential relationship with equilibrium level ($R^2 = 0.94$, P = <0.0001) and thickness ($R^2 = 0.9$, P = <0.0001).

Table 5: Results of the regression analysis of the relationship between the selected variables.

Variables (Relationship)	Model	a	b	A_1	A_2	t_1	t_2	Y_0	R	R^2	P-value
T and CAPE	Linear	- 655.2	61.4	/	/	/	/	/	0.5	/	<0.0006
T and LCL	Linear	- 1508.3	114	/	/	/	/	/	0.7	/	<0.0001
T and EL	ExpGro2	/	/	111135	-1195941	-5.03	-5.04	11102 .7	/	0.5	<0.0003
CAPE and EL	ExpGro2	/	/	-5525	-6292	-7.2	-569.7	11799	/	0.94	<0.0001
CAPE and Thickness	ExpGro2	/	/	-4876	-5787	-6.9	-641	10643	/	0.9	<0.0001

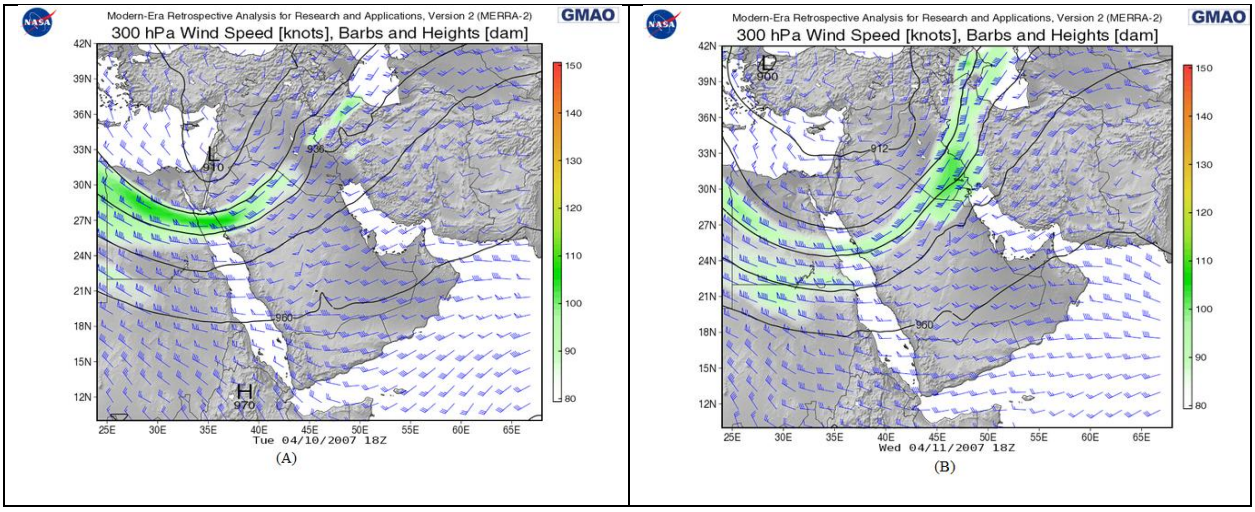
4. Cases Study

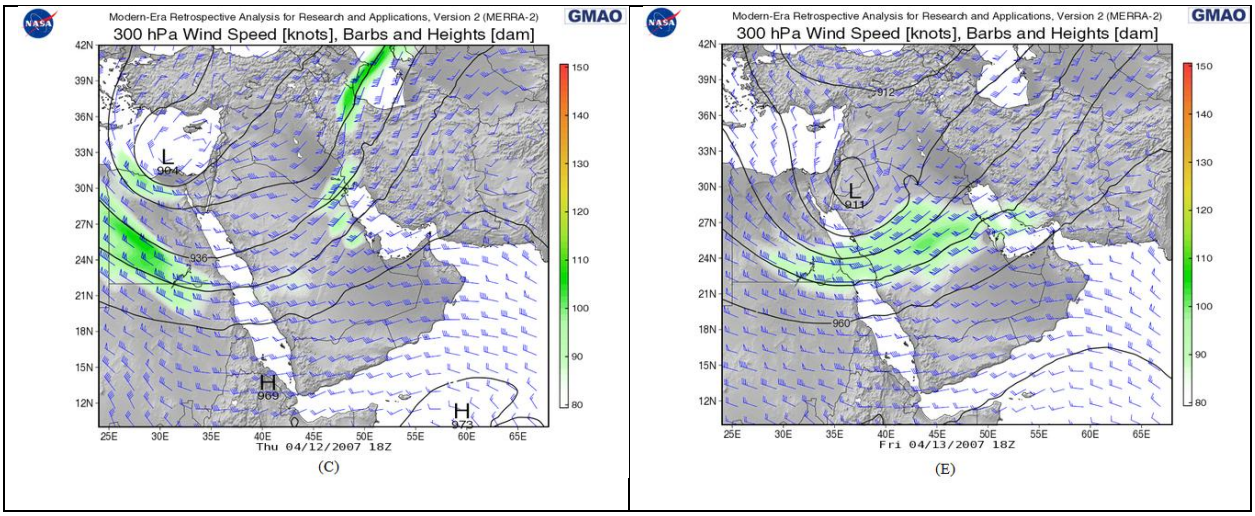
Thunderstorm events were identified based on daily surface observations from the Basra Airport meteorological station. A thunderstorm day can be defined as any day with a reported thunder occurrence in the synoptic records. With incomplete surface observations, days were excluded to ensure data consistency. All identified events were treated with equal weight in the statistical analysis. Thunderstorm events were analyzed using data observed from the Khanaqin weather station at 00:00, 06:00, 12:00, and 18:00 local time for each thunderstorm, including convective rainfall, sea-level atmospheric pressure, geopotential height, relative humidity, and available convective potential energy. This analysis covered both shallow and deep mid-latitude depressions. The case below, representing the longest period of thunderstorms in 30 years, was chosen for synoptic analysis.

4.1. Thunderstorm Case of April 10, 11, 12, and 13, 2007

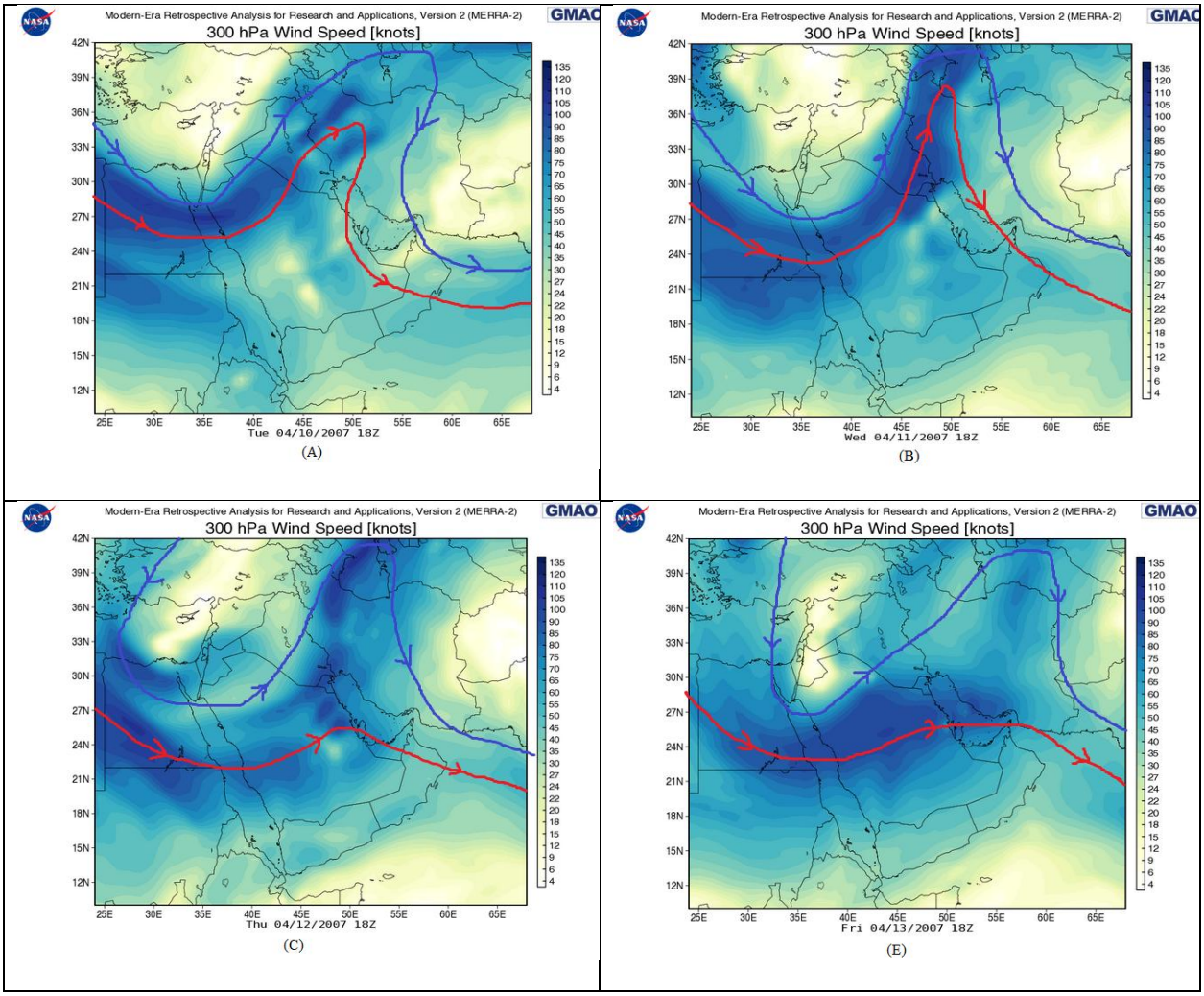
On April 10, 2007, a thunderstorm was recorded at the Basra Airport station at 12:00. The maps in Figure 14 (A-E) show a time series of wind and geopotential height development at the 300 hPa level, which represents the core of the polar and subtropical jet streams. The polar jet stream is responsible for the dynamic control of instability in the Middle East. The polar jet stream contributes to the formation of cyclones and mid-latitude low-pressure systems by generating divergent zones in the upper atmosphere. Instability increases when the polar jet stream extends southward from its position and merges with the subtropical jet stream, leading to increased hydrodynamic instability and deeper low-pressure systems. Panels (A-E) in Figures 14 and 15 show the development of the upper-level wave structure before, during, and after the formation of thunderstorms over Basra.

The maps depict a twin jet stream system across the Middle East, with the subtropical jet stream (STJ, in red) (Figure 15; A-E) stretching from North Africa over the Arabian Peninsula into Iran and the polar jet stream (PJ, in blue) over northern Iraq. This arrangement represents a dynamic pattern known in the literature as the Jet Coupling Pattern, where the spatial overlap between the acceleration and deceleration zones of the two jet streams leads to strong upper-level divergence zones (Uccellini and Johnson, 1979; Keyser and Shapiro, 1986). The jet stream, which extends from North Africa over the eastern Mediterranean to Iraq, is a powerful belt of winds exceeding 65–70 knots over Basra city. The stream is distinguished by a clear, deep Rossby wave trough that moves eastward and is located west of Iraq. Temperatures associated with this low-pressure system have dropped below -40°C at the 300 hPa level as it moves eastward.





529 **Figure 14.** Wind speed and height lines at 300 hpa of April 10, 11, 12, and 13, 2007



530 **Figure 15.** Jet stream at 300 hpa of April 10, 11, 12, and 13, 2007

531

The geopotential height and relative vorticity at 300 hpa (Figure 16: A-E) demonstrate that a reduction in the geopotential height is a clear explanation for the severe rain scenario over Basra. For the atmospheric drop associated with the low atmosphere as well as the relative vorticity between (6-12) 1e-5, we see a clear increase and activity of the relative vorticity in terms of cutting rotation speed and curvature of the vorticity direction, which is an indication of the increase in the movement of air declining counterclockwise and increasing rain activity in the area, specifically above eastern-southern Iraq (phases C and E). The presence of strong positive vortices at upper levels causes air to diverge at that level. To compensate for this divergence, air rises from lower atmospheric levels (updraft). As the air rises, it cools and condenses, increasing the likelihood of cloud formation, thunderstorm development, and rainfall. If sufficient moisture is available at lower levels (which may originate from the Arabian Gulf or the Red Sea), this upper-level weather system will significantly enhance the chances of heavy rainfall and thunderstorms over Basra and the surrounding areas.

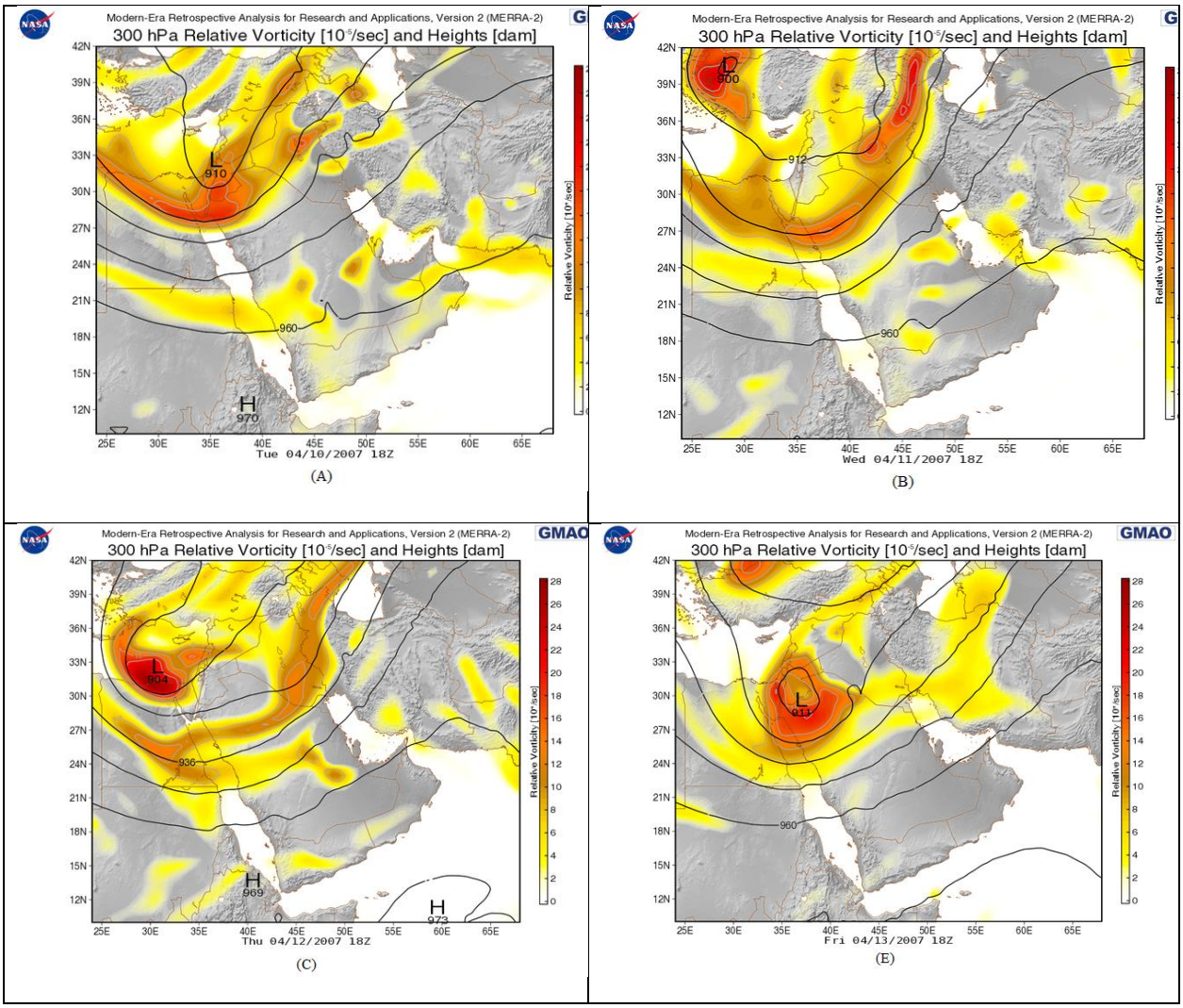


Figure 16. geopotential height and relative vorticity at 300 hpa of April 10, 11, 12, and 13, 2007

The temperature and geopotential height maps at 500 hPa (Figure 17: A-E) show a classic temporal evolution of a deep cold-core upper-level trough over the eastern Mediterranean, Armenia, and Turkey, extending towards northern Iraq and western Iran. Phase A shows an active barocline zone dividing the cold polar air mass to the north from the warm subtropical air to the south, as seen by a high temperature gradient with extremely tight potential height lines over northern and western Iraq. In phase B, the trough deepens significantly and becomes a semi-cut-off upper-

level trough, with temperatures dropping below −23°C at 500 hPa over northern and western Iraq, accompanied by a sharp drop in geopotential height values (≈560 dam). This structure implies a significant increase in vertical instability due to mid-troposphere cooling. In phase C, the trough moves and deepens over the southeastern Mediterranean with a temperature below -25°C at 500 hPa and eastward towards northern and western Iran and eastern and central Iraq with a temperature below -20°C at 500 hPa. In phase E, the trough continues to advance eastward towards western Iran but deepens over northern Saudi Arabia while the study's station records approximately -18°C at 500 hPa, accompanied by a sharp drop in geopotential height values (≈558 dam).

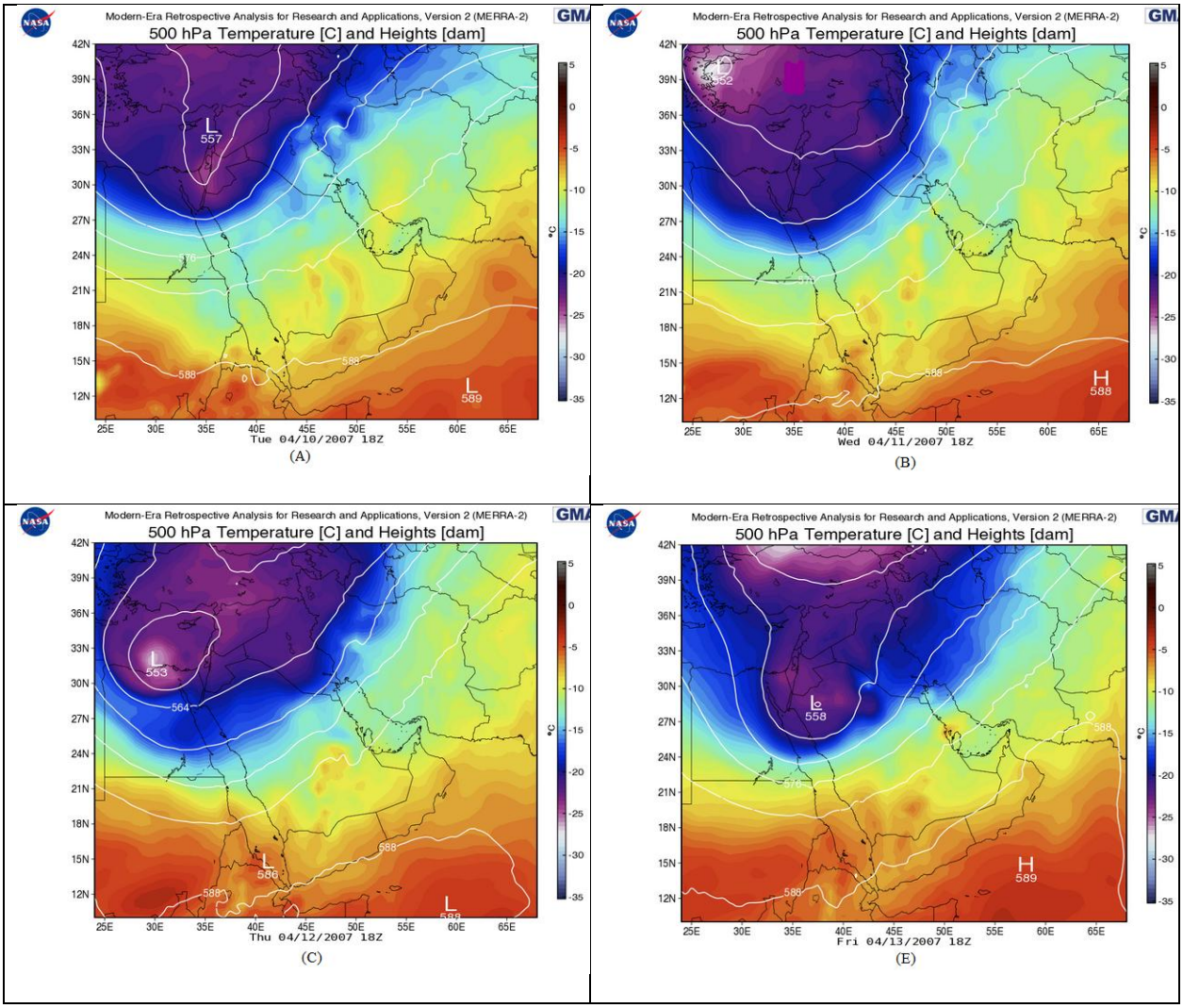


Figure 17. Temperature and height lines at 500 hpa of April 10, 11, 12, and 13, 2007

Surface temperature maps at 2 m (Fig. 18: A-E) show a direct response to the upper-level structure. In phase A, a sharp temperature contrast was observed between a warm, humid air mass extending from the Arabian Gulf and southern Iran and a cooler air mass extending from the eastern Mediterranean, northern Iraq, Iran, and over Turkey—a classic pattern of an active frontal area. In phase B, this temperature gradient intensifies as cold air pushes southward and warm air pushes eastward, leading to the intensification of the frontal region over eastern-southern Iraq. In phase C, Basra city remains within the air mass convergence zone, i.e., the frontogenesis zone, where the probability of both thermal uplift and dynamic uplift increases. In phase E, we observe the rush of warm air mass upwards toward the north, and this indicates the retreat of the low-pressure system (weakening of the cold air mass supply). The polar jet stream and the subtropical jet stream coupled at 300 hPa, coinciding with the emergence of the 500 hPa cold trough

and the surface front. A cold upper-level trough at 500 hPa that accelerated the rate of vertical thermal depreciation, the coupling of the two jet streams at 300 hPa that produced strong upper-level divergence, and an active surface thermal front driven by moisture from the Arabian Gulf are the three governing systems that interacted to produce the Basra city situation, as shown in Figures 15, 16, and 17. Latent instability was transformed into deep, organized thunderstorms as a result of this interaction, which caused the atmospheric column pressure over eastern Iraq to drop, causing the warm, humid air in the lower layers to surge forcefully. This mechanism is similar to what is commonly observed in mid-latitude systems.

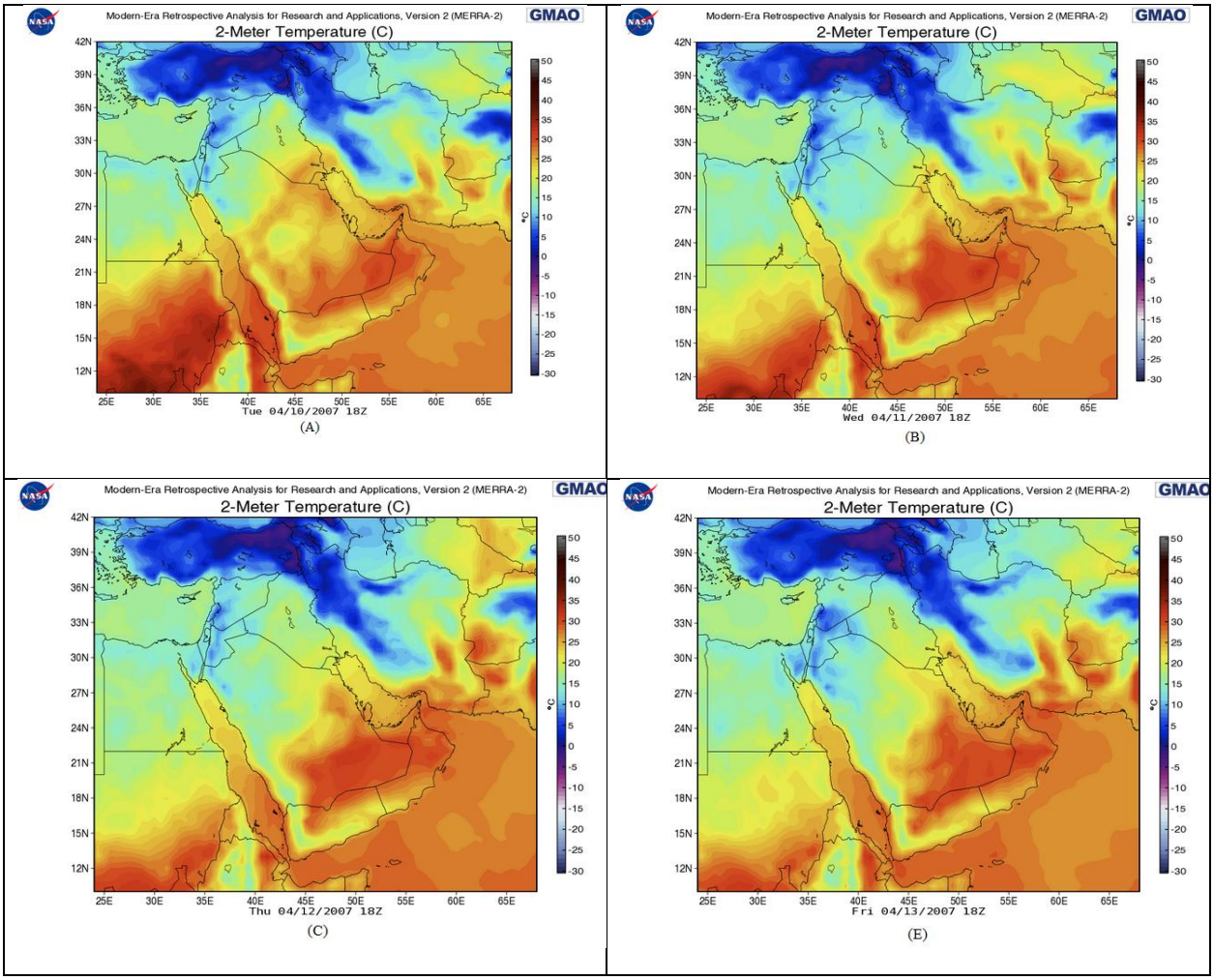


Figure 18. Temperature distribution at a height of 2 meters on April 10, 11, 12, and 13, 2007

The Skew-T/Log-P diagram shown in Figure 19 illustrates the thermal and wind characteristics of the atmosphere over eastern Iraq during the peak of the event (April 10, 2007, 12Z). It clearly reveals that the atmosphere was in a state of deep conditional instability. This instability resulted from a clear divergence between the temperature and dew point curves in the lower and middle layers, contrasted by a strong convergence in the upper layers. This indicates insufficient moisture in the surface layer; a relatively dry low-mid-level air intrusion; relatively high CAPE values (>2000 J kg^{-1}), sufficient to support the development of strong updrafts capable of penetrating the middle and upper troposphere; and a weak or almost nonexistent CIN, meaning that synoptic lift mechanisms (jet + trough) were sufficient to generate convection without the need for intense surface heating. Strong vertical wind shear between 0 and 6 km, resulting from: This pattern is ideal for the development of multicell or supercell-like thunderstorm structures (Weisman & Klemp, 1982; Markowski & Richardson, 2010).

On the evening of April 10, at 18:00, the cloud top temperature exceeded (< −60°C) over the city of Basra, direct evidence of the development of deep convective towers and the arrival of updrafts at the tropopause level. These tops align geographically (location) and temporally with the axis of the active surface front, the updraft zone ahead of the trough at 500 hPa, and the jet stream overlap zone. The notion that large-scale dynamic forcing, as opposed to a localized disturbance, was the cause of the thunderstorms in Basra is supported by this multi-scale consistency.

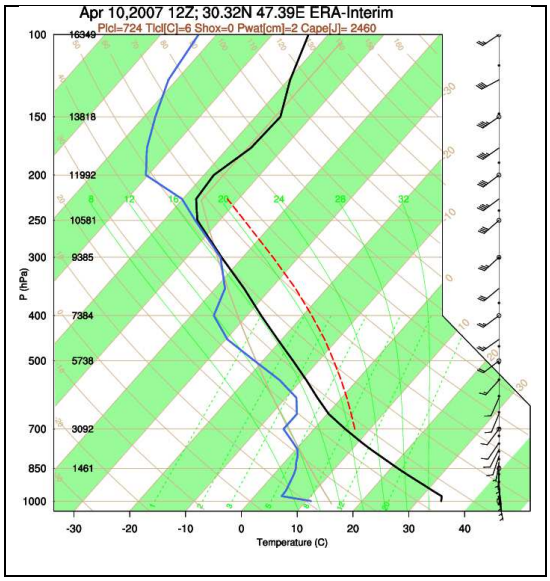


Figure 19. Sounding data Map April 10, 2007

Conflict of Interest Statement

The authors declare that they have no conflicts of interest to report.

Funding Statement

This research did not receive any specific grant from funding agencies in the public, commercial, or not-for-profit sectors.

Author Contributions

"All authors contributed to the study conception and design. Material preparation, data collection and analysis were performed by [Imad Abdulridha Jasim Al-Khulaifawi] and [Aqeel Ghazi Mutar]. The first draft of the manuscript was written by and all authors commented on previous versions of the manuscript. All authors read and approved the final manuscript."

Data Availability

"The datasets generated during and analysed during the current study are available in the [ECMWF/ERA-5] repository, [https://cds.climate.copernicus.eu/datasets/reanalysis-era5-single-levels?tab=download] and [https://cds.climate.copernicus.eu/datasets/reanalysis-era5-pressure-levels?tab=download]"

4. Conclusions

This study provides a comprehensive analysis of thunderstorm activity over the city of Basra Airport station in southern Iraq for the period 1990–2019. This analysis integrates surface observational data, ERA5 reanalysis data, atmospheric instability indices, synoptic analysis, and studies of extreme weather events.

The results showed that the highest frequency of thunderstorms in the Basra Airport station occurs during the spring season, accounting for more than 56.44% of all recorded events. This act is due to the surface temperature increasing, which leads to more convection when unstable conditions are formed. The highest annual frequency of thunderstorms was recorded in 1999, with 22 days of storms. This indicates unusual atmospheric activity associated with increased thermal and humidity instability that year. Most thunderstorms are found to be caused by shallow mid-latitude lows (54.98%), compared to 45.02% for deep lows, reflecting the transitional nature of the region's climate between arid and hot. The K-index ranged between 31 and 35 in most cases (approximately 30.05%), indicating high atmospheric instability. The TT-index ranged between 45 and 50 (46.72%), which is the best indicator for predicting thunderstorms. CAPE values were low for most periods (<2500 J/kg), meaning that strong storms are rare in the region. The work demonstrated that combining the K-index and TT-index provides a more accurate diagnosis of atmospheric instability, which is very useful in the development of early warning systems for thunderstorms, such as Iraq. Correlation analysis revealed moderate to strong positive relationships between temperature, lifting condensation level (LCL), equilibrium level (EL), and convective available potential energy (CAPE), confirming that surface temperature is a key factor in promoting thermal turbulence. Due to increased effective moisture content (from the Arabian Gulf) in the lower atmospheric layers, climate change in arid regions may shorten the duration of thunderstorms and increase their localized intensity, but it also decreases the likelihood of deep, organized storm formation. Higher temperatures enhance the cloud base while also increasing the air's ability to retain water vapor.

References

Ahrens, C. D. (2001). *Essentials of meteorology: An invitation to the atmosphere* (3rd ed.). Brooks/Cole, Thomson Learning.

Al-Ansari, Nadhir. (2013). Management of Water Resources in Iraq: Perspectives and Prognoses. *Engineering*. 05. 667-684. 10.4236/eng.2013.58080

Al-Khulaifawi. I, & Ioshpa. A, (2023). Analysis of Thunderstorm Activity in Iraq and Turkey. *News of the Ural State Mining University*, issue 4(72), pp. 164–169. http://doi.org/10.21440/2307-2091-2023-4-164-169 (in Russian)

Arora, K., Ray, K., Ram, S., & Mehajan, R. (2023). The role of instability indices in forecasting thunderstorm and non-thunderstorm days across six cities in India. *Climate*, 11, 14. https://doi.org/10.3390/cli11010014

Bennett, L. J., Browning, K. A., Blyth, A. M., Parker, D. J., & Clark, P. A. (2006). A review of the initiation of precipitating convection in the United Kingdom. *Quarterly Journal of the Royal Meteorological Society, 132*, 1001–1020. https://doi.org/10.1256/qj.05.54

Bhardwaj, Pankaj & Singh, Omvir & Kumar, Dinesh. (2017). Spatial and temporal variations in thunderstorm casualties over India. *Singapore Journal of Tropical Geography*. 38. doi. 10.1111/sjtg.12201

Buck, A. L. (1981) New equations for computing vapor pressure and enhancement factor, *Journal of Applied Meteorology.* 20(1981) 1527-1532. https://doi.org/10.1175/1520-0450(1981)020<1527:NEFCVP>2.0.CO;2

Cinaroglu, Eda & Unutulmaz, Osman. (2018). A Data Mining Application of Local Weather Forecast for Kayseri Erkilet Airport. *Journal of Polytechnic*. doi. 10.2339/politeknik.391801

Craven, Jeffrey & Jewell, Ryan & Brooks, Harold. (2002). Comparison between Observed Convective Cloud-Base Heights and Lifting Condensation Level for Two Different Lifted Parcels. *Weather and Forecasting*. 17(4). 885-890. doi. 0.1175/1520-0434(2002)017<0885:CBOCCB>2.0.CO;2

Derubertis, D. (2006). Recent trends in four common stability indices derived from U.S. radiosonde observations. *Journal of Climate*, vol. 19, no. 3, pp. 309-323. doi. 10.1175/JCLI3626.1

DiGangi, E.A.; Stock, M.; Lapierre, J. Thunder Hours: How Old Methods Offer New Insights into Thunderstorm Climatology. *Bulletin of the American Meteorological Society,* 2022, 103(2), E548–E569. 10.1175/BAMS-D-20-0198.1

George, J. J. (1960). Weather and Forecasting for Aeronautics. *Academic Press*, Waltham, MA.

Hersbach, H., Bell, B., Berrisford, P., Biavati, G., Horányi, A., Muñoz Sabater, J., Nicolas, J., Peubey, C., Radu, R., Rozum, I., Schepers, D., Simmons, A., Soci, C., Dee, D., & Thépaut, J. N. (2023). ERA5 hourly data on pressure levels from 1940 to present. *Copernicus Climate Change Service (C3S) Climate Data Store (CDS)*. doi: 10.24381/cds.bd0915c6

Humood, B. Y., & Abbas, L. M. (2017). Studying recorded lightning over Iraq for period 1998-2011. *Al-Mustansiriyah Journal of Science*, *28*(3), 1-6. http://doi.org/10.23851/mjs.v28i3.50

Hussain A., N, Thaer O., R, & Zahraa F. R. (2025). Synoptic Analysis of Polar and Subtropical Jet Streams and their Influences on Baghdad City. *An-Najah University Journal for Research – A Natural Sciences*, 40(3), 1-11. 10.35552/anujr.a.40.2.2613

Keyser, D., & Shapiro, M. A. (1986). A review of the structure and dynamics of upper-level frontal zones. *Monthly Weather Review*, 114(2), 452–499. https://doi.org/10.1175/1520-0493(1986)114〈0452:AROTSA〉2.0.CO;2

Khidher, S., & Pilesjö, P. (2014). The effect of the North Atlantic Oscillation on the Iraqi climate 1982–2000. *Theoretical and Applied Climatology*, 122. doi. 10.1007/s00704-014-1327-4

Kianusch et al. (2025). Increasing NWP Thunderstorm Predictability Using Ensemble Data and Machine Learning. http://doi.org/10.48550/arXiv.2502.13316

Krider, E.P. (2021). thunderstorm. *Encyclopedia Britannica*. https://www.britannica.com/science/thunderstorm

Kunz, M. (2007). The skill of convective parameters and indices to predict isolated and severe thunderstorms. Nat. *Hazards Earth Syst. Sci*. 7, 327–342. https://doi.org/10.5194/nhess-7-327-2007

Kunz, M., Wandel, J., Fluck, E., Baumstark, S., Mohr, S., & Schemm, S. (2020). Ambient conditions prevailing during hail events in central Europe. *Natural Hazards and Earth Systems Sciences, 20*, 1867–1887. https://doi.org/10.5194/nhess-20-1867-2020

Lucas, C., Zipser, E. J., & LeMone, M. A. (1994). Convective available potential energy in the environment of oceanic and continental clouds: Correction and comments. *Journal of Atmospheric Science, 51*(24), 3829–3830. https://doi.org/10.1175/1520-0469(1994)051<3829:CAPEIT>2.0.CO;2

Madineni, V. R. & Santhi, Y. & Rajeevan, M. & Rao, S. (2013). Diurnal variability of stability indices observed using radiosonde observations over a tropical station: Comparison with microwave radiometer measurements. *Atmospheric Research*. 124. 21–33. doi. 10.1016/j.atmosres.2012.12.007

Markowski, P., & Richardson, Y. (2010). Mesoscale meteorology in midlatitudes. *Wiley-Blackwell*. 10.1002/9780470682104

Miller, R. C., Bidner, A., & Maddox, R. A. (1972). The use of computer products in severe weather forecasting (the SWEAT index). *Air Weather Service Aerospace Sciences Review*. AWS RP 105-2, No: 72-1, 2-9.

Mondal, U., Panda, S. K., Das, S., & Sharma, D. (2022). Spatio-temporal variability of lightning climatology and its association with thunderstorm indices over India. *Theoretical and Applied Climatology, 149*, 273–289. https://doi.org/10.1007/s00704-022-04032-5

National Oceanic and Atmospheric Administration. (2016). El Niño and La Niña: Frequently Asked Questions. *NOAA Climate.gov*. Retrieved from https://www.climate.gov/news-features/understanding-climate/el-nino-and-la-nina-frequently-asked-questions

NSSL. (2020). SEVERE WEATHER 101 / Thunderstorm Basics. *National Severe Storms Laboratory, NOAA*. https://www.nssl.noaa.gov/education/svrwx101/thunderstorms/

National Weather Service (NWS). (2022). National Weather Service: Definition of atmospheric variables, atmospheric stability indicies. https://www.weather.gov/ffc/gloss2

Rabbani, Khan & Das, Someshwar & Panda, Suprita & Kabir, Alamgir & Mallik, Muhammad. (2021). Physical and Dynamical Characteristics of Thunderstorms Over Bangladesh Based on Radar, Satellite, Upper-Air Observations, and WRF Model Simulations. *Pure and Applied Geophysics.* 178(2). 10.1007/s00024-021-02847-3

Saha, U., Maitra, A., Midya, S. K., & Das, G. K. (2014). Association of thunderstorm frequency with rainfall occurrences over an Indian urban metropolis. *Atmospheric Research, 138*, 240–252. https://doi.org/10.1016/j.atmosres.2013.11.021

Sawaisarje, G. & Singh, Gauravendra & Chaudhari, Hemantkumar & Ranalkar, Manish & Das, Sunit. (2025). Improving thunderstorm and lightning prediction using a novel hybrid index and machine learning techniques: a case study in Northeast India. *Meteorology and Atmospheric Physics*. 137(4), 10.1007/s00703-025-01080-0

Shmeter, S. M. (1972). Fizika konvektivnykh oblakov [Physics of Convective Clouds]. Leningrad: *Gidrometeoizdat*. 231 p. (in Russian)

Showalter, A. K. (1953). A stability index for forecasting thunderstorms. *Bull. Amer. Meteor. Soc*, 34, 250-252. 10.1175/1520-0477-34.6.250

Singh, O., & Bhardwaj, P. (2017). Spatial and temporal variations in the frequency of thunderstorm days over India, Weather, 74(4), 138–144. doi. 10.1002/wea.3080

Sultan A. G. Climate, its elements and changes. Baghdad: Baghdad Publishing House, 1986. 480p. (in Arabic).

Trapp, R. J. (2013). Mesoscale-convective processes in the atmosphere. Cambridge University Press. https://doi.org/10.1017/CBO9781139047241

Tyagi, Ajit. (2007). Thunderstorm climatology over Indian region. *Mausam*. 58. 189-212. doi. 10.54302/mausam.v58i2.1204

U.S. Department of Defense. (1990). The use of the skew T, log P diagram in analysis and forecasting. Technical rept. https://unidata.github.io/MetPy/latest/_static/USAF_SkewT_manual.pdf

Uccellini, L. W., & Johnson, D. R. (1979). The coupling of upper and lower tropospheric jet streaks and implications for the development of severe convective storms. *Monthly Weather Review*, 107(5), 682–703. https://doi.org/10.1175/1520-0493(1979)107

Umakanth, N., Satyanarayana, G. C., Simon, B., Rao, M. C., & Babu, N. R. (2020). Long-term analysis of thunderstorm-related parameters over Visakhapatnam and Machilipatnam, India. *Acta Geophysica, 68*, 921–932. https://doi.org/10.1007/s11600-020-00431-2

Viceto, C.; Marta-Almeida, M.; Rocha, A. Future climate change of stability indices for the Iberian Peninsula. *Int. J. Climatol*. 2017, 37, 4390–4408. https://doi.org/10.1002/joc.5094

Wang, P. K. (2013). "Observation of clouds", in *Physics and Dynamics of Clouds and Precipitation*. https://doi.org/10.1017/CBO9780511794285

Weisman, M.L.; Klemp, J.B. (1982). The dependence of numerically simulated convective storms on vertical wind shear and buoyancy. *Mon. Weather. Rev*, 110(6), 504–520. 10.1175/1520-0493(1982)110<0504:TDONSC>2.0.CO;2

Xu, D., You, X., & Xia, C. (2019). Assessing the spatial-temporal pattern and evolution of areas sensitive to land desertification in North China. *Ecological Indicators, 97*, 150-158. https://doi.org/10.1016/j.ecolind.2018.10.005

Ye, B., Genio, A.D.D., Lo, K.K.W. (1998) CAPE variations in the current climate and in a climate change. *J. Clim*., 11(8), 1997–2015. https://doi.org/10.1175/1520-0442

Zahraa et al. (2021). Thunderstorm dynamic analysis based on total precipitation over Iraq. Journal of Engineering Science and Technology. 16. 62-70.